Published in final edited form as:
Cancer Discov. 2024 November 11; 15(2): 427–443. doi:10.1158/2159-8290.CD-24-0263.

Survivin promotes stem cell competence for skin cancer initiation

Sara Canato[1,*], **Rahul Sarate**[2,*], **Sofia Carvalho-Marques**[1,*], **Raquel Maia Soares**[1], **Yura Song**[2], **Sara Monteiro-Ferreira**[1], **Pauline Vieugué**[2], **Mélanie Liagre**[2], **Giancarlo Grossi**[3], **Erik Cardoso**[1], **Christine Dubois**[2], **Edward M Conway**[4], **Silvia Schenone**[3], **Adriana Sánchez-Danés**[1,#,$], **Cédric Blanpain**[2,#,$]

[1]Champalimaud Research, Champalimaud Centre for the Unknown, Lisbon, Portugal

[2]Laboratory of Stem Cells and Cancer, Université Libre de Bruxelles (ULB), Brussels, Belgium.

[3]Pharmacy Department, University of Genoa, Genoa, Italy.

[4]Centre for Blood Research, Life Sciences Institute, Department of Medicine University of British Columbia, Vancouver, Canada.

Abstract

Stem cells (SCs) and not progenitors (Ps) act as cells of origin of Basal Cell Carcinoma (BCC). The mechanisms promoting BCC formation in SCs or restricting tumour development in Ps are currently unknown. In this study, we transcriptionally profiled SCs and Ps and found that Survivin, a pleiotropic factor that promotes cell division and inhibits apoptosis was preferentially expressed in SCs. Using genetic gain and loss of function mouse models, we showed that Survivin deletion in oncogene-expressing SCs prevents BCC formation. Survivin overexpression renders Ps competent to BCC formation by promoting cell survival and division while preventing apoptosis and differentiation. We identified SGK1, as a key downstream factor of Survivin, and its inhibition prevents BCC formation. This study uncovers the role and mechanisms by which Survivin regulates the competence of SCs to initiate BCC formation promoting the survival of oncogene-expressing SCs and self-renewing division while restricting differentiation and apoptosis.

Introduction

Homeostasis of the skin interfollicular epidermis (IFE) is maintained by heterogenous populations of stem cells (SCs) and progenitors (Ps) located in the basal compartment. Lineage tracing studies have shown that the Krt14-CREER mice target SC and Ps, while Inv-CREER mice preferentially target Ps (1–3).

[$]denotes co-corresponding authors, **Corresponding authors:** Adriana Sánchez-Danés: adriana.sanchezdanes@research.fchampalimaud.org, Champalimaud Research, Champalimaud Center for the Unknown, Avenida Brasília 1400-038 Lisboa, Portugal, Cédric Blanpain: Cedric.Blanpain@ulb.be, Université Libre de Bruxelles (ULB), 808, route de Lennik, Bat GE, G2 4.205, 1070 Bruxelles, Belgium.
[*]denotes co-first authors
[#]denotes co-last authors

Conflict of interest statement
The authors declare no potential conflicts of interest

Europe PMC Funders Author Manuscripts

Europe PMC Funders Author Manuscripts

BCC is the most frequent cancer in humans (4). BCC arises upon constitutive activation of the HH signaling pathway through either *Patched 1 (Ptch1)* loss of function or *Smoothened (Smo)* gain of function mutations (4). In mice, BCC arises preferentially from SCs located in the IFE and infundibulum (5–7). Within the IFE, SCs and Ps present different competence to induce BCC formation. Activation of the HH signaling pathway through deletion or activation of the active form of *Smoothened (SmoM2)* in SCs using the Krt14-CREER lead to BCC formation (2). In contrast, oncogenic activation of HH pathway with the same oncogenic hit in Ps using the Inv-CREER lead to the formation of lesions that are frozen in their preneoplastic stage and do not progress into invasive BCC (2). The mechanisms that confer the competence to BCC formation in the epidermal SCs and restrict BCC development in Ps remain unresolved.

In this study, we have assessed the mechanisms that confer the competence of SCs to BCC initiation in mice. Using transcriptional profiling, we uncovered that *Birc5/Survivin* is preferentially expressed in oncogene-expressing SCs compared with oncogene-expressing Ps. Using gain and loss of function of *Survivin in vivo*, we showed that Survivin expression is required for BCC initiation by promoting cell survival and proliferation, as well as, restricting terminal differentiation of oncogene-expressing cells. Finally, we showed that Survivin mediates BCC initiation through upregulation of Sgk1, uncovering a new pharmacological approach to prevent BCC formation.

Results

Survivin is expressed in SmoM2 expressing epidermal SCs

As previously shown, overexpression of *SmoM2* in epidermal SCs using *Krt14-CREER* leads to BCC formation whereas *SmoM2* expression in epidermal Ps using *Inv-CREER* leads to lesions that are frozen in the preneoplastic stages and fail to progress into invasive BCC (Fig 1A)(2). To identify the molecular changes associated with *SmoM2* expression in SCs and Ps, we performed bulk RNA-seq of FACS isolated oncogene-expressing (SmoM2-YFP+) basal cells (β4-integrin high) 8 weeks following tamoxifen administration in *Krt14-CREER/SmoM2-YFP* (SCs enriched, thereafter referred as *Krt14/SmoM2*) and *Inv-CREER/SmoM2-YFP* (Ps enriched, thereafter referred as *Inv/SmoM2*).

Oncogene-expressing SCs upregulated genes associated with SC proliferation (eg. *Sox9*), stemness (eg. *Tbx1*) (8,9), keratinocyte proliferation (eg. *Nrg1, Tgfa, Krt6a, Krt16*) (10–12), embryonic hair follicle progenitors (EHFP) (eg. *Runx1*) (5), cytoskeleton and invasion (eg. *Myo1B, Myo5B, Palld*) (8)) (Fig 1B). In addition, genes negatively regulating apoptosis (eg. *Birc5, Fos, Jun*) (13,14) were also enriched in the *Krt14/SmoM2* expressing cells (Fig 1B). In contrast, the *Inv/SmoM2* expressing cells were enriched for genes involved in epidermal differentiation (eg. *Notch4, Satb1, Tgm2, Tgm3*), lipid metabolism and lipid synthesis (eg. *Elovl3, Elovl6, Fa2h, Fads6, Scd1*) (Fig 1C), as previously described in Inv WT targeted cells (1).

Among the genes downregulated in Ps expressing SmoM2, *Baculoviral Inhibitor of apoptosis repeat containing 5 (Birc5)* also known as Survivin, attracted our attention as Ps present increased apoptosis compared to SCs following SmoM2 expression (2). Survivin

is a member of the inhibitors of apoptosis family also involved in the control of mitosis, as it is part of the chromosomal passenger complex, and is expressed in several cancer types (14). *In situ* hybridization confirmed the high levels of Birc5/Survivin expression in BCCs derived from *Krt14/SmoM2* mice compared to the low levels observed in the *Inv/SmoM2*-derived dysplasia (Fig 1D). These data suggest that the upregulation of Birc5/Survivin in oncogene-expressing SCs and not in Ps could regulate the competence of SCs to initiate BCC development.

Survivin deletion in SCs prevents BCC formation

To assess whether Survivin expression in SCs is required for BCC development, we performed the conditional deletion of *Survivin* together with the activation of *SmoM2* in the SCs using *Krt14-CREER/SmoM2/Survivin* $^{fl/fl}$ (referred thereafter as *SmoM2/Survivin cKO*) mice that allowed to induce *Survivin* deletion together with activation of oncogenic *SmoM2* following tamoxifen administration (Fig. 2A and Supplementary Fig. S1A). The persistence of oncogene-expressing cells and the pathological phenotype (hyperplasia, dysplasia, invasive BCC) of oncogene-expressing cells was assessed by confocal microscopy on whole mount tail epidermis (2). Deletion of *Survivin* in *SmoM2/Survivin cKO* lead to a strong decrease of the tumour burden and a rapid loss of oncogene-expressing cells (Fig 2B-D and Supplementary Fig. S1B-C). In contrast, in the presence of Survivin in *Krt14/SmoM2* mice, most of the clones expressing *SmoM2* survived over time and progressed into BCC as previously described (Fig. 2B-D and Supplementary Fig. S1B-C)(2). Only some of the rare persisting oncogene-expressing clones in the *SmoM2/Survivin cKO* progressed into small BCCs, accounting for around 6% of the initially induced clones compared to 21% in *Krt14/SmoM2* mice 12 weeks upon tamoxifen administration (Fig. 2D and Supplementary Fig S1 B-C). These rare small BCCs found in the *SmoM2/Survivin cKO* mice expressed Survivin as demonstrated by immunostaining for Survivin expression and *Survivin in situ* hybridization, indicating that the small fraction of BCC arising in *SmoM2/Survivin cKO* correspond to escaper cells that did not recombine and delete *Survivin* floxed alleles (Supplementary Fig. S1 D-E).

To understand the causes of the loss of oncogene-expressing cells following Survivin deletion, which could be already observed 1 week upon tamoxifen administration, we first assessed the basal clone size. We observed that the *Krt14/SmoM2* clones presented more basal cells (1.8 vs 1.2 cells per clone) by 1 week following tamoxifen administration and 6.6 vs 2.1 cells per clone by 2 weeks compared to *SmoM2/Survivin cKO* (Fig. 2E). In addition, upon *Survivin* deletion around 30% of the clones by week 1 and 2 did not have basal attachment, indicating that these cells were differentiating leading to delamination and clone loss (Fig.2 F-G). In contrast, only 8% and 4% of the *Krt14/SmoM2* clones expressing Survivin were delaminating at 1 and 2 weeks respectively. Immunostaining for *SmoM2* and the differentiation marker keratin 10 (KRT10) 2 weeks following tamoxifen administration showed a higher number of SmoM2 basal cells expressing KRT10 following Survivin deletion (Supplementary Fig. S1F-G). In *Krt14/SmoM2* clones, KRT10 was expressed in suprabasal layers whereas Survivin was expressed in the proliferative basal compartment, as shown by colocalization of Survivin with Aurora Kinase B, a protein required in chromosome segregation and cytokinesis (Supplementary Fig S1H-I) (15).

In addition, cell proliferation was strongly decreased following *Survivin* deletion, as shown by the decrease in Ki67 positive cells (56% and 8% of Ki67+ cells in *Krt14/SmoM2* and *SmoM2/Survivin cKO* mice) 4 weeks after tamoxifen administration (Fig. 2H-I).

To assess whether in addition to the promotion of differentiation and delamination, an increase of apoptosis following *Survivin* deletion (14) participates in the loss of oncogene-expressing clones, we quantified the proportion of cleaved caspase 3 (CC3) expressing cells in the presence and in the absence of *Survivin* following SmoM2 expression. We found that *Survivin* deletion strongly increased the number of clones positive for CC3, as well as, the proportion of apoptotic cells per clone from 2.6% to 6% by 4 weeks after tamoxifen administration and from 1.2% to 4% by 8 weeks following tamoxifen administration in *Krt14/SmoM2* and *SmoM2/Survivin cKO* mice respectively. (Fig. 2J-L). We did not observe cells co-expressing CC3 and Survivin in lesions from *Krt14/SmoM2* mice (Supplementary Fig. S1J).

The most prevalent mutation leading to BCC in humans is the loss of function of the tumour suppressor gene *Ptch1* (4). To assess if the key role of Survivin in promoting the survival of SmoM2-expressing cells is conserved across the different mutations promoting oncogenic hedgehog signalling, we performed the conditional deletion of *Ptch1* and *Survivin* in *Krt14-CREER/Ptch1* $^{fl/fl}$*/Survivin* $^{fl/fl}$ mice (thereafter referred as *Krt14/Ptch1KO/Survivin KO*) (Fig. 2M). Similarly to what we found in SmoM2 mice, we found that the deletion of Survivin in the context of *Ptch1* deletion also strongly inhibited the formation of BCC (Fig. 2N-O). Altogether, these data indicate that Survivin expression in the SCs is critically important for BCC formation by promoting oncogene-expressing cells proliferation and survival through the restriction of apoptosis and terminal differentiation.

Survivin overexpression confers to Ps the competence to initiate BCC development

As the survival of *SmoM2*-targeted cells in Ps and in SCs following *Survivin* loss of function decreases overtime, we assessed whether *Survivin* gain of function could rescue the survival of *SmoM2* expressing Ps and render the Ps competent to initiate BCC formation. To this end, we generated a new genetic mouse model allowing the overexpression of *Survivin* in the basal cells targeted by *SmoM2* in a doxycycline inducible manner (Supplementary Fig. S2A-B and Supplementary Materials&Methods). In this new genetic model, cells that overexpress Survivin could be identified by mCherry expression due to the presence of a Survivin-IRES-mCherry cassette (Supplementary Fig. S2A-B). To test the effect of Survivin overexpression in Ps upon oncogenic activation, we generated the *Inv-CREER/Rosa-SmoM2-YFP/Krt14rtTA/tetO-Survivin-IRES-mCherry, thereafter* referred as *Inv/SmoM2/Survivin GOF* (Fig.3A). Specifically, the *Inv/SmoM2/Survivin GOF* mice were treated with doxycycline to overexpress Survivin starting for the duration of the experiment and one week before tamoxifen administration, the latter leading to *SmoM2* expression (Supplementary Fig. S2C).

Upon Survivin overexpression, the oncogene-targeted Ps gave rise to BCCs 12% of the clones were BCCs and 26% of the clones were BCCs, at 8 and 12 weeks following SmoM2 expression respectively. Whereas in the absence of Survivin overexpression, oncogene-targeted Ps did not progress from dysplasia into BCCs as previously reported

(2) (Fig 3B-D and Supplementary Fig. S2D). In addition, Survivin overexpression led to a stabilisation in the survival of oncogene-targeted cells after the second week following oncogene expression, while the clone number in *SmoM2* targeted Ps continued to decrease overtime as previously described (2) (Fig. 3E and Supplementary Fig. S2E). We did not find differences in the number of proliferative cells or basal clone size in BCCs arising from SC in *Krt14/SmoM2* model compared to BCCs arising from Ps upon Survivin and SmoM2 expression in *Inv/SmoM2/Survivin GOF* mice (Supplementary Fig. S2F-G).

To define the mechanism(s) by which Survivin overexpression confers the competence of Ps to induce clonal persistence and BCC formation, we first assessed whether Survivin overexpression promotes clonal expansion in oncogene-targeted Ps. We found that Survivin overexpression led to an increase in basal clone size at different time points following oncogene expression (Fig 3F). We then assessed whether Survivin overexpression prevented the elimination of oncogene-targeted Ps by apoptosis (2). Upon Survivin overexpression, the proportion of clones expressing CC3 decreased, as well as, the % of CC3 positive cells per clone 8 weeks following tamoxifen administration (Fig.3G-I).

Next, we assessed if this increase in clone size could be also mediated by a difference in cell proliferation. To this end, we assessed oncogene-targeted cell proliferation by quantifying the number of proliferative cells per clone. We found an increase in Ki67 positive cells following Survivin overexpression in the *Inv/SmoM2/Survivin GOF* clones compared to the *Inv/SmoM2*, indicating that proliferation was enhanced following Survivin overexpression (Fig.3J-K).

To assess whether clonal survival and BCC formation following Survivin overexpression was the consequence of a change in cell fate outcome favouring symmetric cell division, we performed short-term 5-bromo-2'-deoxyuridine (BrdU) pulse chase experiments. To this end, we administrated a low dose of BrdU to mark a minority of dividing cells and assessed cell fate outcome 3 days later by quantifying the relative proportion of basal and suprabasal localization of BrdU doublets. We found that Survivin overexpression led to an increase in the proportion BrdU doublets made of two basal cell (from 52% in *Inv/SmoM2* to 68% in *Inv/SmoM2/Survivin GOF*) and a decrease in the divisions that led to doublets of differentiated cells (from 14% *Inv/SmoM2* to 3% in *Inv/SmoM2/Survivin GOF*) compared to the Ps indicating that upon Survivin overexpression promotes self-renewing division and decrease in differentiation in SmoM2-expressing Ps, similar to what we found in oncogene-targeted SCs (2) (Fig.3L-M).Survivin overexpression in wild type skin did not lead to the formation of BCC or alter the differentiation potential of the basal cells of the epidermis (Supplementary Fig S2 H-I).

We then assess whether the promotion of BCC formation by Survivin overexpression in Ps is also found following *Ptch1* deletion. To this end, we generated *Inv-CREER/Ptch1$^{fl/fl}$/Krt14-rtta/teto-Survivin-IRES-mCherry* mice (thereafter referred as *Inv/Ptch1-cKO/Survivin GOF*) (Fig.3N). Survivin overexpression also led to BCC formation arising from the Inv targeted Ps following *Ptch1* deletion (Fig.3O-P), demonstrating that the promotion of BCC formation by Survivin overexpression in Ps is conserved across different oncogenic mutations activating hedgehog pathways.

Europe PMC Funders Author Manuscripts

Altogether this data indicate that *Survivin* overexpression confers the competence of oncogene-targeted Ps to initiate BCC formation by enhancing proliferation and promoting self-renewing divisions, as well as, by inhibiting apoptosis and preventing differentiation in preneoplastic lesions arising from Ps.

Survivin promotes stem cell-like properties during skin homeostasis

To determine whether Survivin expression controls stemness in skin SCs in the absence of oncogene expression, we first assess whether Survivin is upregulated in normal SCs compared to Ps. Quantitative RT-PCR showed that *Survivin* expression is upregulated in normal SCs (*Krt14-CREER/Rosa-YFP* clones, thereafter referred as *Krt14/YFP*) compared to Ps (*Inv-CREER/Rosa-YFP* clones, thereafter referred as *Inv/YFP*) in homeostatic conditions (Supplementary Fig S3A).

Using gain and loss of Survivin function, we assess whether Survivin expression controls stemness in skin SC *in vivo* during homeostatic conditions. Deletion of *Survivin* together with expression of the reporter gene YFP in SCs using the *Krt14* promoter in *Krt14-CREER/Rosa-YFP/Survivin fl/fl* mice thereafter referred as *Krt14/YFP/Survivin cKO* (Supplementary Fig S3B) led to an increase in clonal loss over time compared to clones expressing wild type Survivin (*Krt14-CREER/Rosa-YFP* mice) from 62.8 % to 20.2% by 12 weeks following tamoxifen administration (Supplementary Fig S3C-D). The Krt14/YFP clones that persisted were bigger than the clones of *Krt14/SmoM2/Survivin cKO* (3.4 basal cells versus 2.4 basal cells) at 12 weeks following tamoxifen administration (Supplementary Fig S3E).

In contrast, overexpression of Survivin in Ps in homeostatic condition using the *Inv-CREER/Rosa-YFP/Krt14rtTA/tetO-Survivin-IRES-mCherry*, thereafter referred as *Inv/YFP/Survivin GOF* (Supplementary Fig S3F and G) led to an increase in clonal persistence from 8.1% to 30% and an increase in the clone size (basal cells 2.5 in WT versus 3.6 basal cells upon Survivin overexpression) at 12 weeks following tamoxifen administration (Supplementary Fig S3H-J). These data show that Survivin deletion in SCs lead to a clonal behaviour similar to Ps, while overexpression of Survivin in Ps lead to a clonal behaviour similar to SCs, indicating that Survivin mediates stemness in the skin basal compartment in the absence of oncogene expression.

Pharmacological inhibition of Survivin prevents the progression of preneoplastic lesions into BCCs

To define the role of Survivin during the progression of preneoplastic lesions into invasive BCCs, we first assessed Survivin expression in hyperplasia and dysplasia derived from SCs and Ps. Survivin was highly expressed at the mRNA and protein level in hyperplasia and dysplasia derived from SC in the *Krt14/SmoM2* mice compared to lesions derived from Ps in the *Inv/SmoM2* mice, (Supplementary Fig. S4A-B). To test whether Survivin can promote the conversion of preneoplastic lesions into invasive BCCs in *Krt14/SmoM2* and *Inv/SmoM2/SurvivinGOF* mice, we treated mice with Survivin inhibitor (YM155) at 8 weeks upon tamoxifen administration (Fig.4A), a timepoint when the majority of lesions are dysplasia that progress into BCC (Supplementary Fig S1 C and Fig 3D). We could only

treat the mice for 10 days, as long-term administration of this inhibitor induced systemic toxicity that requests the termination of the experiments. Treatment of *Krt14/SmoM2* and *Inv/SmoM2/SurvGOF* mice with Survivin inhibitor led to a decrease in the number of lesions and tumour burden, and also to a decreased number of lesions that progressed into BCC from around 60% to 20% in *Krt14/SmoM2* mice and from 45% to less than 10% in the *Inv/SmoM2/Survivin GOF* mice (Fig.4 B-D and Supplementary Fig S4C-D). To define the underlying mechanisms that restrict the progression of these preneoplastic lesions into BCCs, we performed immunostaining for markers of apoptosis (CC3) and proliferation (Ki67) upon Survivin inhibitor administration. We observed an increase in apoptosis - from 0.3% to 11.37% of CC3+ in Krt14/SmoM2 and from 3.5% to 17.4% in *Inv/SmoM2/ Survivin GOF* following inhibitor administration (Fig 4 E-G). In addition, administration of Survivin inhibitor decreased proliferation from 35.7% of Ki67 positive cells to 23.3% in *Krt14/SmoM2* mice and from 15.2% to 7.8% in *Inv/SmoM2/SurvGOF* mice (Fig 4 H-I). In addition, immunostaining for the differentiation marker KRT10 showed that in the untreated tumorigenic lesions KRT10 was mainly observed in suprabasal differentiated cells and that the treatment with Survivin inhibitor led to the expression of KRT10 in the basal cells (Fig4 J-K). Altogether, these results indicate that administration of Survivin inhibitor decreases the progression of the preneoplastic lesions into BCC by promoting apoptosis and differentiation, as well as, decreasing proliferation.

To determine whether overexpression of Survivin in SmoM2-expressing preneoplastic lesions derived from Ps allow them to progress into BCC, we administrated tamoxifen to activate the SmoM2 in Ps in *Inv/SmoM2/SurvivivnGOF* mice. Three weeks after tamoxifen administration when the majority of the lesions became hyperplasia and some dysplasia, we administered doxycycline to overexpress Survivin (Supplementary Fig S4 E). Following Survivin overexpression, 20% of the lesions progressed into BCC at 8 weeks following tamoxifen administration, compared to 0 % in the absence of Survivin overexpression (Supplementary Fig. S4 F-H and Fig 3D), similar to the proportion of BCC observed when Survivin is overexpressed before tamoxifen administration (Supplementary Fig. S4 H and Supplementary Fig 1C). However, the total number of clones was reduced by 50% compared to Survivin overexpression prior to tamoxifen administration (Supplementary Fig S4 I). These results further confirm that Survivin overexpression promotes progression of preneoplastic lesions into BCC.

Survivin overexpression prevents Ps differentiation into different epidermal lineages

As Survivin overexpression confers the competence of Ps to initiate BCC formation following oncogenic HH mutations by promoting self-renewing divisions and restricting apoptosis and differentiation, we next assessed whether the cell state changes induced by SmoM2 expression in Ps is affected by Survivin overexpression. To this end, we performed scRNAseq on FACS isolated *SmoM2-YFP* cells from *Inv/SmoM2* (n=8046 cells) and *Inv/SmoM2/SurvivinGOF* mice (n=6056 cells) 8 weeks after tamoxifen administration. We performed unsupervised clustering on individual samples using Seurat and annotated different clusters based on known markers gene expression for each condition previously described by scRNA-seq of skin epidermis (16–19). In both conditions, we identified different clusters based on the expression of specific genes that can be classified into distinct

SC/P clusters, SC/P G0 (eg. *Igfbp2, Stfa3, Sparc*), SC/P G2-M (eg. *Mki67, Top2a, Cenpa*), differentiated basal cells of the scale (Scale Diff) (eg.*Krt36, Krt84*) and differentiated basal cells of the interscale (Interscale Diff)(eg. Krt2, Krt10), sebaceous gland (SG) (eg. *Mgst1, Scd1*), committed cells (committed diff)(eg. *Krt17, Mt2, Krtdap*), infundibulum progenitor (INF prog) (eg. *Foxc1, Aldha3a1, Lrig1*), infundibulum differentiated cells (INF Diff) (eg. *Sox9, Rflnb, Lmo1*), EHFP reprogramming cells that are found in oncogene-targeted cells during BCC formation (eg. *Lgr5, Lhx2, Ptch1*)(5)(Fig. 5A-B, Supplementary Fig. S5 A-I and Supplementary Fig. S6 A-I). Our comparative analysis between *Inv/SmoM2* and *Inv/SmoM2/SurvivinGOF* showed an increase in the proportion of differentiated cells in the absence of Survivin overexpression (Fig.5 A-B). Data integration using Seurat showed that Survivin overexpression led to the disappearance of the cell cluster only observed in the *Inv/SmoM2* condition (Fig. 5C-D). Sub clustering of this *Inv/SmoM2* specific cluster reveals that it was composed by cluster committed towards Infundibulum differentiation (eg. *Ly6d, Defb6*), cluster committed towards IFE differentiation (eg. *Krt10, Krtdap*) and cluster committed towards SG differentiation (eg.*Scd1, Mgst1*) (Fig 5E-F). To validate the results of the scRNA seq, we performed immunofluorescence and *in situ* hybridization (RNAscope) analysis using markers specific for the different clusters committed towards differentiation. Immunofluorescence showed that Survivin overexpression restricts the expression of IFE differentiation marker KRT10 and the SG differentiation marker SCD1 in *Inv/SmoM2* cells at a similar level as *SmoM2-expressing* SCs (Fig. 5G-H). *Defb6 in situ* hybridization (ISH) revealed that Survivin overexpression restricted the expression of *Defb6* in oncogene-targeted Ps, similar as found in oncogene-targeted SC (Fig. 5G-H). Altogether these data reveal that Survivin overexpression in oncogene-targeted Ps prevents their differentiation into various epidermal lineages.

Survivin overexpression promotes cell division, survival and prevents apoptosis and differentiation

To further refine the molecular mechanisms by which Survivin expression promotes the competence of basal cells to induce BCC formation upon SmoM2-expression we performed bulk RNA sequencing of SCs and Ps in the absence (Ps and SCs Survivin KO) or in the presence (SCs and Ps Survivin GOF) of Survivin expression. To this end, we FACS isolated basal cells of the interfollicular epidermis (α6-integrin high and CD34 negative) and excluding the bulge SC (α6-integrin high and CD34 positive) expressing SmoM2 fused to YFP from *Inv-SmoM2, Inv/SmoM2/SurvivinGOF, Krt14/SmoM2, SmoM2/Survivin cKO* mice and performed bulk RNA-seq in two independent biological samples (Supplementary Fig. S7 A-B). We compared the transcriptome of these different populations and defined different signatures: (a) the SC specific signature as genes upregulated in SmoM2-expressing SC compared to SmoM2-expressing Ps (up *Krt14/SmoM2* vs *Inv/Smo*), (b) the Survivin regulated gene signature in Ps as genes upregulated in SmoM2-expressing Ps upon Survivin overexpression vs SmoM2-expressing Ps (up *Inv/SmoM2/SurivivinGOF* vs *Inv/SmoM2*) and (c) the Survivin regulated gene signature in SCs as genes downregulated upon Survivin deletion in SmoM2-expressing SCs compared to SmoM2-expressing SCs (up *Krt14/SmoM2* vs *SmoM2/Survivin cKO*).

We found that 82 genes were commonly upregulated upon Survivin expression (common genes across the three different gene signatures), that were enriched for genes regulating survival, proliferation, including *Tgfa, Aqp3, Heg1*, ligands of the ERB receptors (*Nrg1* or *Hbegf*), members of the MAPK signaling pathway (*Map2K3, Map3K14* and *Map3K6*) or the Serum glucocorticoid regulated kinase 1 (Sgk1), a kinase that promotes survival and proliferation and inhibits apoptosis (20) (Fig 6A-C).

In order to validate that the absence/downregulation of Survivin expression is associated with keratinocyte differentiation as demonstrated by our previous scRNAseq data analysis, we assessed the genes commonly upregulated in absence of Survivin expression in three gene signatures (d) the P specific signature as genes upregulated in SmoM2-expressing Ps compared to SmoM2-expressing SCs (up *Inv/SmoM2* vs *Krt14/Smo*), (e) the genes upregulated in absence of Survivin expression in the SmoM2-expressing Ps (up *Inv/SmoM2* vs *Inv/SmoM2/Survivin GOF*) and (f) the genes upregulated upon Survivin deletion in SCs (up *SmoM2/Survivin cKO* vs *Krt14/SmoM2*). We found 241 genes commonly upregulated in the abovementioned signatures involved in epidermal differentiation (*eg. Krt2, Nrp1*), lipid metabolism and lipid synthesis (*eg. Elovl3, Elovl6, Fa2H, Lpl, Lss, Mgll, Scd1*) associated with keratinocyte and skin barrier function (21) (Fig 6D-F).

Altogether our results identified the genes modulated by *Survivin* expression in the context of SmoM2-expressing cells that may promote oncogene-targeted cell proliferation, survival and preventing their terminal differentiation.

SGK 1 is a Survivin regulated gene essential for BCC formation

As Survivin is essential for BCC formation, we assessed whether among the genes regulated by *SmoM2* in a Survivin dependent manner, there are genes that promote BCC formation and could be targeted pharmacologically, as an alternative to the use of Survivin inhibitor. Among the 82 genes that were commonly upregulated by Survivin expression across all three experimental conditions tested, Serum and glucocorticoid-regulated kinase 1 (Sgk1) appears as a potential candidate gene regulating Survivin-mediated stemness during BCC formation (Fig.6 A-C). Sgk1 shares structural and functional similarities with the AKT family of kinases, is expressed in several cancer types and has been involved in cancer cell proliferation, apoptosis and migration (20). Immunohistochemistry showed that SGK1 is not expressed in hyperplasia, starts to be expressed in dysplasia, and persists at BCC stage in *Krt14/SmoM2* and *Inv/SmoM2/Survivin GOF* mice, but not in preneoplastic lesions from *Inv/SmoM2* mice (Fig.6G and Supplementary Data Fig S8A).

To assess the role of SGK1 in regulating BCC formation, we treated *Krt14/SmoM2* and *INV/SmoM2/Survivin GOF* mice 8 weeks following TAM administration with SGK 1 inhibitor (SGK1 Inh, SI113) (22) for 4 weeks (Fig 7A). Interestingly, SGK 1 inhibitor treatment led to a decrease in the density of *SmoM2*-expressing lesions and a decrease in the number of dysplastic lesions that progressed into BCC, resulting in a 10-fold and 27-fold decrease in tumour burden in the *Krt14/SmoM2* and *INV/SmoM2/Survivin GOF* mice respectively compared to the control group (Fig 7 B-D and Supplementary Fig. S8 B-C).

We next assessed the mechanism by which SGK1 inhibitor was preventing BCC formation. As SGK1 has been described to regulate apoptosis and proliferation, we performed immunostaining for the apoptotic marker (CC3) and assessed proliferation using Ki67 expression in *Krt14/SmoM2* and *Inv/SmoM2/SurvivinGOF* mice. SGK1 inhibition led to an increase in the number of apoptotic cells per lesion from 1.6% to 6.2% in *Krt14/SmoM2* and from 3.5% to 12% in *Inv/SmoM2/Survivin GOF* following SGK1 inhibitor administration (Fig 7 E-G). In addition, the number of proliferative Ki67+ cells was decreased from 20.9% to 9.2 %in the *Krt14/SmoM2* and 18.3% to 13.3% in the *Inv/SmoM2/Survivin GOF* following SGK1 inhibition (Fig 7H-I). Moreover, SGK1 inhibition promoted differentiation of the basal cells in the tumorigenic lesions as indicated by the increase in KRT10 expression in basal compartment (KRT14-expressing cells) (Fig 7J-K and Supplementary Fig 8D). To uncover whether SGK1 inhibition impacts on Survivin expression, we assessed Survivin expression in lesions from *Krt14/SmoM2* mice treated with SGK1 inhibitor and controls. We found that SGK1 inhibition led to a decrease in the proportion of tumorigenic cells expressing Survivin, suggesting that SGK1 can promote Survivin expression (Supplementary Fig S8 E-F).

Altogether these experiments demonstrate that SGK1 inhibition inhibits BCC formation by decreasing cell proliferation while promoting apoptosis and differentiation, phenocopying the effect of Survivin deletion or pharmacological inhibition and demonstrating that pharmacological SGK1 inhibition represents as an alternative strategy to prevent BCC formation.

Discussion

In this study, we define the mechanisms underlying the relative competence of SCs and Ps to mediate BCC initiation and identify Survivin as a key factor that confers SC competence to initiate BCC formation.

Transcriptional profiling of SCs and Ps identify Survivin as being strongly upregulated in SCs compared to Ps in the mouse epidermis upon HH signaling pathway activation. Loss of Survivin function in SCs in the presence or in the absence of oncogene expression leads to a rapid disappearance of normal SCs and oncogene-targeted SCs and decreases their ability to initiate BCC. Conversely, Survivin overexpression in Ps decreases their rapid clonal loss and promotes their ability to initiate BCC formation following SmoM2 expression. Interestingly, Survivin was also identified as upregulated in human keratinocyte SCs that give rise *in vitro* to colonies that are more proliferative and clonogenic called holoclones, compared to colonies composed of committed progenitors that are non-clonogenic referred as meroclones and paraclones (23), suggesting that Survivin expression might be a hallmark of epidermal SC across species.

Single cell analysis combined with immunostaining and functional experiments reveal that Survivin expression increases cell proliferation, stimulates self-renewing divisions, restricts apoptosis and terminal differentiation of oncogene-targeted cells promoting clonal persistence, clonal expansion and tumor initiation (Supplementary Fig S9).

The role of Survivin in tumour progression has been described in many tumour types, where its expression has been correlated with enhanced cell proliferation and survival. For this reason several Survivin inhibitors have been developed and are currently tested in clinical trials (14). The role of Survivin in tumour progression has been reported in SHH medulloblastoma, a pediatric brain tumour that arises upon constitutive activation of the HH signaling pathway during cerebellar development. That study reported that in established SHH medulloblastoma, Survivin deletion or inhibition led to medulloblastoma shrinkage in a grafting heterotopic model (24). Whereas the role of Survivin in tumor progression has been previously described, our study now shows that Survivin expression is essential at the earliest stage of tumor initiation, and that confers to SCs the relative competence of tumor formation. Our data also indicates that Survivin overexpression confers stemness to more committed cells and overcomes their inability to mediate BCC formation. Survivin overexpression acts in the epidermis similarly as inflammation promotes tumorigenesis in the intestine, inducing dedifferentiation of non-SCs and promoting their ability to acquire tumour-initiating capacity (25). Our data also show that short term administration of Survivin inhibitor leads to shrinkage and elimination of preneoplastic lesions and prevents BCC progression.

Finally, we have identified SGK1 inhibition as a new strategy to block the promotion of cell survival and cell proliferation mediated by SmoM2 in a Survivin dependent manner, and to prevent BCC initiation. Several SGK1 inhibitors have recently been developed and described to lead to tumour shrinkage alone or in combination with other treatment options in a variety of tumour types (20). Our data show that SGK1 inhibition can prevent the conversion of preneoplastic lesions into invasive tumours, representing an alternative to the use Survivin inhibitor in the prevention of BCC progression.

Material and Methods

Mice

Krt14-CreER(26) (RRID:IMSR_JAX:005107) transgenic mice were kindly provided by E. Fuchs, Rockefeller University. Inv-CreER mice were generated in Cédric Blanpain laboratory (6) (RRID:IMSR_JAX:019380). *Ptch1*$^{fl/fl}$, Rosa/YFP and Rosa/SmoM2-YFP mice were obtained from the JAX repository (RRID:IMSR_JAX:012457; RRID:IMSR_JAX:006148; RRID:IMSR_JAX:005130). K14rtTA transgenic mice (27) were provided by E. Fuchs (RRID:IMSR_JAX:008099). The Survivin fl/fl animals were kindly provided by E.M. Conway.

Mouse colonies were maintained in a certified animal facility in accordance with European guidelines for the laboratory animal use and care based on the 2010/63/EU Directive. Experiments involving mice presented in this work were approved by the Animal Welfare and Ethics Body, Direção-Geral da Alimentação e Veterinária (DGAV,Portuguese Authority) under protocol number 2019/012 and Comité d'Ethique du Bien Être Animal (Université Libre de Bruxelles) under protocol number 483N.

Skin tumour induction

For tumour induction 1.5-months-old mice were used. *Krt14/SmoM2, SmoM2/Survivin cKO, Krt14/PtchcKO, Krt14/PtchcKO/Surivivin cKO* mice received an intraperitoneal injection of 0.1 mg (0.5 mg/ml) of tamoxifen (ref. T5648-0005, Sigma). *Inv/SmoM2, Inv/SmoM2/SurvivinGOF, Inv/PtchcKO and Inv/PtchcKO/Survivin GOF* and received one intraperitoneal injection of 2.5 mg (12.5 mg/ml) of tamoxifen to achieve similar levels of recombination in the different models. *Inv/SmoM2/SurvivinGOF and Inv/PtchcKO/Survivin GOF* mice received an intraperitoneal injection (2mg/ml in PBS) weekly followed by doxycycline in drinking water (2 mg/ml daily)until the animal was euthanized. Mice were sacrificed and analysed at different time points following tamoxifen administration. SmoM2 animals were heterozygous for the SmoM2 mutation in the Rosa Locus. Ptch1cKO were Ptch1 fl/fl, homozygous for the floxed allele. Animals showing low or patchy mCherry expression were excluded from this study

The tail skin and ventral skin were used in our analysis. Specifically, in the SmoM2 model the tail skin was analyzed, as in this model BCC arises in the tail, paws and ear (Youssef, Nat Cell Biol 2010).

While the ventral skin was the one used in the analysis of the PtchcKO model, as tumours in this model arise in the ventral and back skin and ears (Youssef, Nat Cell Biol 2012).

Lineage tracing experiments during skin homeostasis

For the lineage tracing experiments 1.5-months-old mice were used. Krt14/YFP mice received an intraperitoneal injection of 0.1 mg (0.5 mg/ml) of tamoxifen (ref. T5648-0005, Sigma) and I*nv-CreER/Rosa-YFP* received one intraperitoneal injection of 2.5 mg (12.5 mg/ml) of tamoxifen to achieve similar levels of recombination in the different models. *Inv/YFP/SurvivinGOF* mice first received an intraperitoneal injection followed by administration of doxycyline in drinking water of 2mg/ml until the animals were euthanized (every week) and 1 week after the first injection of doxycycline they received an intraperitoneal injection of 2.5 mg (12.5 mg/ml) of tamoxifen. Mice were sacrificed and analysed at different time points following tamoxifen administration. All mice were heterozygous for *Rosa-YFP*. Animals showing low or patchy mCherry expression were excluded from this study.

SGK1 inhibitor administration

SGK 1 inhibitor (SI113) was kindly provided by Silvia Schenone and Giancarlo Grossi (University of Genoa). During SGK1 inhibitor treatment, mice received SGK 1 inhibitor at a concentration of 50mM twice per day by intraperitoneal injection for 4 weeks. SGK inhibitor was dissolved in 0.9% NaCl solution.

Survivin inhibitor administration

During Survivin inhibitor treatment, mice received 5mg/kg/day of YM155 (Selleckchem #S1130) by continuous subcutaneous infusion using micro-osmotic pump (model 1002, Alzet). Survivin inhibitor was dissolved in 1x PBS solution.

Whole-mounts of tail epidermis

Whole mounts of tail epidermis were performed as previously described (2)

Specifically, pieces of tail were incubated for 1 hour (h) at 37 °C in EDTA 20 mM in PBS in a rocking plate, then using forceps the dermis and epidermis were separated and the epidermis was fixed for 30 min in PFA 4% in agitation at room temperature and washed 3 x with PBS.

For the immunostaining, tail skin pieces were blocked with blocking buffer for 3 h (PBS, horse serum 5%, Triton 0.8%) in a rocking plate at room temperature. After, the skin pieces were incubated with primary antibodies diluted in blocking buffer overnight at 4 °C, the next day they were washed with PBS-Tween 0.2% for 3 × 10 min at room temperature, and then incubated with the secondary antibodies diluted in blocking buffer for 3 h at room temperature, washed 2 × 10 min with PBS-Tween 0.2% and washed for 10 min in PBS. Finally, they were incubated in Hoechst (1:1000) diluted in PBS for 30 min at room temperature in the rocking plate, washed 3 × 10 min in PBS and mounted in DAKO mounting medium supplemented with 2.5% Dabco (Sigma). Primary antibodies used were the following: Goat anti-GFP (1:800, ref. ab6673, Abcam, RRID:AB_300798), Rat anti-β4-integrin (1:500, ref. 553745, BD Pharmingen, RRID:AB_395027),Rabbit anti-caspase-3 (1:600, ref. AF835, R&D, RRID:AB_2243952), Rabbit anti-Ki67 (1:1000, ab15580, abcam, RRID:AB_443209), rabbit anti-Survivin (1:800, ref. 2808, Cell Signaling, RRID:AB_2063948). R&D Systems Secondary antibodies used were the following: anti-goat, anti-rat, anti-rabbit conjugated to AlexaFluor488 (Goat, ref A-11055, Invitrogen, RRID:AB_2534102), to rhodamine Red-X (Rat, ref 712-295-153, Jackson Immunoresearch, RRID:AB_2340676; Rabbit, 711-295-152, Jackson Immunoresearch, RRID:AB_2340613) and to AlexaFluor647 (Rat, ref 712-605-153, Jackson Immunoresearch, RRID:AB_2340694; Rabbit, 711-605-152, Jackson Immunoresearch, RRID:AB_2492288). Images were acquired using Z-stacks with an inverted confocal microscope LSM 980 (Carl Zeiss).

Immunostaining in sections

The tail in the SmoM2 model and ventral skin in the *Ptch1*cKO model were embedded in optimal cutting temperature compound (OCT, ref. 4583 Sakura) and cut into 7 to 8 μm frozen sections using CM3050S Leica cryostat (Leica Microsystems). Frozen sections were dried and fixed with 4% PFA for 10 min at room temperature and blocked with a blocking buffer (PBS 1x, Horse serum 5%, BSA 1%, Triton 0.2%) for 1 h. Skin sections were incubated with primary antibodies overnight at 4ºC, washed with PBS 1x for 3 x 5 min, and then incubated with secondary antibodies and Hoechst (1:1000, ref H3570, Invitrogen) for 1 h at room temperature in agitation. Finally, sections were washed with PBS 1x for 3 x 5 min at room temperature and mounted in DAKO mounting media (Ref. 237-C056330-2, Dako). Primary and secondary antibodies used were diluted in blocking buffer. Primary antibodies used were the following: Goat anti-GFP (1:500, ref. ab6673, Abcam, RRID:AB_300798), Rat anti-β4-integrin (1:500, ref. 553745, BD Pharmingen, RRID:AB_395027), Rabbit anti-Caspase-3 (1:600, ref. AF835, R&D Systems, RRID:AB_2243952), Rabbit anti-Krt10 (1:4000, PRB-159P, Covance/

IMTEC, RRID:AB_291580), Rabbit anti-Aurora Kinase B (1:200, ab2254, Abcam, RRID:AB_302923) and Chicken anti-GFP (1:400, ab13970, Abcam, RRID:AB_300798). Secondary antibodies used were the following: anti-goat, anti-rat, anti-rabbit, anti-chicken conjugated to AlexaFluor488 (Goat, ref A-11055, Invitrogen, RRID:AB_2534102), to rhodamine Red-X (Rat, ref 712-295-153, Jackson Immunoresearch, RRID:AB_2340676; Rabbit, 711-295-152, Jackson Immunoresearch, RRID:AB_2340613) and to AlexaFluor647 (Rat, ref 712-605-153, Jackson Immunoresearch, RRID:AB_2340694; Rabbit, 711-605-152, Jackson Immunoresearch, RRID:AB_2492288). Images were acquired using inverted confocal microscope LSM 980 (Carl Zeiss).

Brdu proliferation experiments

For proliferation assay, mice received intraperitoneal injection of 3mg/ml Brdu (ref. B9285, Merck). Mice were sacrificed after 3 days and whole-mount staining for the tail was performed. The pieces of tail were first stained for anti-GFP (1:800, ref. ab6673, Abcam, RRID:AB_300798) and then, skin pieces were washed 3 x 10 min with a washing buffer (PBS 1x, Tween 0.2%) and fixed for 15min in PFA 4%. Skin pieces were then washed 3 x 10 min and incubated 20 min with HCL 1M at 37ºC. Skin pieces were incubated with AlexaFluor647 mouse anti-BrdU (1:200, ref. 560209, BD Pharmagen, RRID:AB_1645615) overnight at room temperature under agitation. Finally, skin pieces were washed 3 x 10min with PBS 1x, incubated with Hoechst (1:1000) and washed 3 x 10min with PBS 1x and mounted in DAKO mounting media. Images were acquired using Z-stacks using an inverted confocal microscope LSM 980 (Carl Zeiss).

Immunohistochemistry

For SGK1 immunohistochemistry, 5 μm paraffin sections were deparaffinized, rehydrated, followed by antigen unmasking performed for 20min in Sodium citrate (pH6). Rabbit anti-SGK1 antibody (1:100, ref PA5-87746, Invitrogen, RRIB: AB_2804383) was used.

In situ hybridization/RNA FISH

For *In situ* hybridization of *Birc5* 5 μm of PFA-fixed paraffin sections were deparaffinized and the in-situ protocol was performed according to the manufacturer instructions (Advanced Cell diagnostics). The following mouse probes were used: Mm-Birc5 cat. No. 422701 and Mm-Defb6 cat. No. 430141. *In situ* hybridization of Defb6 performed according to the manufacturer instructions (RNAscope™ Multiplex Fluorescent V2 Assay, ACD bio). Immunofluorescence staining for GFP+ *Defb6 in situ* hybridization: first we performed *In situ* hybridisation for Defb6 on section and then performed regular immunofluorescence staining for GFP which includes steps of blocking the tissue for 1 h at room temperature and overnight antibody incubation at 4° C and secondary antibody for 1 h to detect the signal of GFP.

Analysis of clone survival, size and apoptosis

Quantification of the proportion of surviving clones (persistence) and the basal clone size were determined by counting the number of SmoM2-positive cells in each clone using orthogonal views of the whole-mount tail epidermis in the interscale region of interfollicular

Europe PMC Funders Author Manuscripts

epidermis as described in (1) (2). Number of active-caspase-3-, Ki67-, Survivin- cells and positive-BrdU-doublets cells in each clone were also quantified using orthogonal views of the whole-mount tail epidermis. β4-integrin staining was used to classify the clone according to their location in basal or suprabasal layers.

FACS isolation of tumours and Bulk RNA sequencing

Tail skins were separated from the tail bone and incubated overnight in trypsin at 4°C (Gibco). The next day the epidermis was separated from the dermis and incubated for 20 min in trypsin on a rocking plate. Trypsin was neutralized by adding DMEM containing 10% Chelex FBS. Epidermal solution was collected and resuspended in a blocking buffer (DPBS 1x, EDTA 5mM, chelated FBS 5%) filtered with a 70μm followed by a 40 μm strainer. The obtained single cell solution was then centrifuged at 500g for 10min at 4°C and the pellet was resuspended in FACS buffer (DPBS 1x, EDTA 2mM, chelated FBS 2%). Cells were stained using Rat Biotin anti-CD34 (1:50, ref 13-0341-85, eBioscience, RRID: AB_466426) and Rat anti-α6-integrin-PE (1:600, ref 12-0495-83, eBioscience, RRID: AB_891474) followed by the secondary antibody APC-streptavidin (1:400, ref 554067, BD Pharmingen, RRID:AB_10050396), and Hoechst 33342 (1:4000,ThermoFisher, ref. H3570, 10mg/mL). Cells were sorted at the Flow Cytometry Platform (Champalimaud Foundation and Université Libre de Bruxelles) using BD FACSAria Fusion Cell Sorter with nozzle 85 μm and filter 2.0μm. Forward versus side scatter (FSC vs SSC) gating was used to identify the cells of interest based on size and granularity.

RNA extraction, Reverse transcription-PCR and quantitative real-time PCR

RNA extraction was performed using RNeasy micro kit (ref. 74004, Quiagen) according to the manufacturer's instructions. cDNA was synthesized using High-capacity RNA-to-cDNA kit (ref. 4387406, ThermoFisher) according to the manufacturer's instructions. qRT-PCR amplifications were performed in a QuantStudio™ 5 Real-Time PCR machine (Bio-rad) using 384 well plate with NZYSupreme qPCR Green Master mixture (ref. MB44003, NZYTech) and a set of primers (mouse BIRC5, F:5'-CACCTTCAAGAACTGGCCCTT-3', R:5'-TTCCCAGCCTTCCAATTCCTTA-3'; mouse HPRT, F:5'-GCAGTACAGCCCCAAAATGG-3', R:5'-TCCAACAAAGTCTGGCCTGT-3') according to the manufacturer's instructions. The fold difference in gene expression was calculated by the relative quantification method using the mathematical equation 2^{-ddCT}.

Bulk RNA sequencing

10.000-200.000 FACS cells were collected directly in the lysis buffer provided by the manufacturer (RNAeasy Microkit, Quiagen) and RNA extraction was then carried out according to the manufacturer's protocol. Indexed cDNA libraries were obtained using the Ovation Solo RNA-seq Systems (NuGen) following manufacturer's recommendations. The multiplexed libraries were loaded on flow cells and sequences were produced using a NovaSeq 6000 S2 Reagent Kit (200 cycles from Novaseq 6000 System, Illumina) on a NovaSeq 6000 System (Illumina).

Reads were mapped against the mouse reference genome (Grcm38/mm10) using STAR software (28) (RRID:SCR_004463) to generate read alignments for each sample.

Annotations for the reference genome (Mus_musculus.GRCm38.87.gtf) were obtained from ftp.Ensembl.org. After transcripts assembling, gene level counts were obtained using HTseq-count (29) (RRID:SCR_011867) and normalized to 20 millions of aligned reads. Genes with individual sample expression levels lower than 10 and replicate average expression levels lower than 20 were filtered out. The fold changes of average gene expression for the replicates were used to calculate the level of differential gene expression between different cell populations. Genes with an expression fold change greater or equal to 2 were considered as up-regulated and those with an expression fold change lower or equal to 0.5 were considered down-regulated.

scRNA sequencing

We sorted cells for $\alpha6^{High}$/$CD34^{-}$/YFP^{+} from INV-SmoM2 (n=8046) and INV-SmoM2-SurvivinGOF mice. Total10,000 cells were loaded onto each channel of the Chromium Single Cell 3′ microfluidic chips (V2-chemistry, PN-120232, 10X Genomics) and barcoded with a 10X Chromium controller according to the manufacturer's recommendations (10X Genomics). RNA from the barcoded cells was subsequently reverse transcribed, followed by amplification, shearing 5′ adaptor and sample index attachment. The libraries were prepared using the Chromium Single Cell 3′ Library Kit (V3-chemistry, PN-120233, 10X Genomics) and sequenced on an Illumina Novaseq 6000 (paired-end 100bp reads).

Single cell transcriptomic data analysis

Sequencing reads were aligned and annotated with the mm10-2020-A reference dataset as provided by 10X Genomics and demultiplexed using CellRanger (v.6.1.1) (30) (RRID:SCR_023221)with default parameters. Further downstream analyses were carried out individually for each of two sample (Inv/SmoM2, Inv/SmoM2/SurvivinGOF).

Quality control and downstream analysis were performed using the Seurat R package(31) (RRID:SCR_016341) (v4.2.0). For each sample, all of the cells passed the following criteria: showed expression of more than 2000 and less than 6000 unique genes and had less than 10% UMI counts belonging to mitochondrial sequences. Read counts were normalized by *NormalizeData()* function of Seurat, with parameter 'normalization.method = "LogNormalize" and scale.factor=10000'. A PCA for each sample was calculated using the scaled expression data of the most variable genes (identified as outliers on a mean/variability plot, implemented in the *FindVariableGenes()*). UMAP calculation(32) and graph-based clustering were done for each sample using the appropriate functions from Seurat (default parameters) with the respective 30 PCA results as input.

The clusters expressing immune cell (*Cd74, Cd52*) and fibroblast (*Vim*) markers are excluded and dimentionality has been recaluclated. The final resolutions were set to 0.5 after testing a range from 0.2 to 0.7. Given that the obtained clustering sensitivity for a given resolution is dependent on the number of cells of that subpopulation in each respective sample, we swept over the same range of resolutions for the other samples, to assure the presence/absence of described clusters in all samples. Selected resolutions are the best to reflect the biological heterogeneity between different cell types. A Wilcoxon rank-sum test was used to define marker genes for each cluster using the *FindAllMarkers()* function.

Europe PMC Funders Author Manuscripts

Benjamini–Hochberg FDR correction for potential cluster marker genes across all samples using the p.adjust method in R and only markers expressed in at least 25% of cells of the cluster, having an average log2-fold change of at least 0.25 were reported.

For visualization and comparison between different samples, we integrated *Inv/SmoM2* and *Inv/SmoM2/Survivin GOF* using the Seurat package's standard CCA-MNN based data integration workflow. Feature selection was performed using the *FindVariableFeatures* function from Seurat with default parameters, selecting the 2000 most variable genes. Canonical correlation analysis (CCA) followed by integration anchors selection was then performed on the selected features using the *FindIntegrationAnchors()* function from Seurat, taking the first 30 dimensions from the CCA into account, as described on the standard workflow of Seurat (RRID:SCR_ 016341). These anchors were then used to integrate the data with the *IntegrateData()* function. Following the annotation of clusters, clusters sharing the same cell identities were merged into a single cluster. This merging process was performed after confirming that there were no differences in terms of gene expression between these clusters with the same cell identity. The assessment of gene expression was based on both well-known marker genes and marker genes determined using the Wilcoxon rank-sum test.

On the individual and integrated datasets, to identify cell proliferation stages, the S-phase and G2/M-phase scores were computed by *CellCycleScoring()* function, implemented in Seurat.

Statistical analysis

All statistical analysis were performed using GraphPad Prism v.8.0.1(www.graphpad.com) (RRID:SCR_002798) software. Data are expressed as mean ± s.e.m. Normality was tested using Shapiro-Wilk Test. For the database that followed normality, Pvalues were estimated with unpaired t-test for two experimental groups or for multiple comparison two-way ANOVA. For the dataset that did not follow the normal distribution, Pvalues were calculated with the Mann-Whitney test. For all the figures, the number of mice and the number of clones is indicated in the figure body or figure legend.

The sample size was chosen based on previous experience in the laboratory, for each experiment to yield high power to detect specific effects. No statistical methods were used to predetermine sample size.

Investigators were not blinded to mouse genotypes during experiments. Researchers were not blinded when performing imaging and quantification.

Supplementary Material

Refer to Web version on PubMed Central for supplementary material.

Acknowledgments

We thank the Champalimaud and ULB animal facility, ULB genomic core facility (F. Libert and A. Lefort), and Champalimaud ABBE platform, J.M.Vanderwinden and LiMif for the help with microscopy.

A.S.D, S.C and R.M.S is supported by QuantOCancer Project Horizon European Union's Horizon 2020 programme (grant agreement No 810653). S.C.M is supported by Fundação para a Ciência e Tecnologia (2021.05801.BD). This project is supported by a Fundação para a Ciência e Tecnologia grant to A.S.D (PTDC/MED-ONC/5553/2020). R.S, M.L. are supported by Télévie. C.B. is supported by WEL Research Institute, FNRS, TELEVIE, Fond Erasme, Fondation Contre le Cancer, ULB Foundation and European Research Council.

Data availability

Data associated with this study have been deposited in the NCBI Gene Expression Omnibus under accession number GSE277554 (bulk RNA sequencing) and GSE277555 (single cell RNA sequencing).

References

1. Mascre G, Dekoninck S, Drogat B, Youssef KK, Brohee S, Sotiropoulou PA, et al. Distinct contribution of stem and progenitor cells to epidermal maintenance. Nature. 2012; 489 (7415) 257–62. [PubMed: 22940863]
2. Sanchez-Danes A, Hannezo E, Larsimont JC, Liagre M, Youssef KK, Simons BD, Blanpain C. Defining the clonal dynamics leading to mouse skin tumour initiation. Nature. 2016; 536 (7616) 298–303. DOI: 10.1038/nature19069 [PubMed: 27459053]
3. Blanpain C, Simons BD. Unravelling stem cell dynamics by lineage tracing. Nat Rev Mol Cell Biol. 2013; 14 (8) 489–502. [PubMed: 23860235]
4. Epstein EH. Basal cell carcinomas: attack of the hedgehog. Nat Rev Cancer. 2008; 8 (10) 743–54. DOI: 10.1038/nrc2503 [PubMed: 18813320]
5. Youssef KK, Lapouge G, Bouvree K, Rorive S, Brohee S, Appelstein O, et al. Adult interfollicular tumour-initiating cells are reprogrammed into an embryonic hair follicle progenitor-like fate during basal cell carcinoma initiation. Nat Cell Biol. 2012; 14 (12) 1282–94. [PubMed: 23178882]
6. Youssef KK, Van Keymeulen A, Lapouge G, Beck B, Michaux C, Achouri Y, et al. Identification of the cell lineage at the origin of basal cell carcinoma. Nat Cell Biol. 2010; 12 (3) 299–305. [PubMed: 20154679]
7. Dlugosz A. The Hedgehog and the hair follicle: a growing relationship. J Clin Invest. 1999; 104 (7) 851–3. DOI: 10.1172/JCI8416 [PubMed: 10510325]
8. Larsimont JC, Youssef KK, Sanchez-Danes A, Sukumaran V, Defrance M, Delatte B, et al. Sox9 Controls Self-Renewal of Oncogene Targeted Cells and Links Tumor Initiation and Invasion. Cell Stem Cell. 2015; 17 (1) 60–73. [PubMed: 26095047]
9. Chen T, Heller E, Beronja S, Oshimori N, Stokes N, Fuchs E. An RNA interference screen uncovers a new molecule in stem cell self-renewal and long-term regeneration. Nature. 2012; 485 (7396) 104–8. DOI: 10.1038/nature10940 [PubMed: 22495305]
10. Hegde GV, de la Cruz C, Giltnane JM, Crocker L, Venkatanarayan A, Schaefer G, et al. NRG1 is a critical regulator of differentiation in TP63-driven squamous cell carcinoma. Elife. 2019; 8 doi: 10.7554/eLife.46551 [PubMed: 31144617]
11. Vassar R, Fuchs E. Transgenic mice provide new insights into the role of TGF-alpha during epidermal development and differentiation. Genes Dev. 1991; 5 (5) 714–27. [PubMed: 1709129]
12. Leigh IM, Navsaria H, Purkis PE, McKay IA, Bowden PE, Riddle PN. Keratins (K16 and K17) as markers of keratinocyte hyperproliferation in psoriasis in vivo and in vitro. Br J Dermatol. 1995; 133 (4) 501–11. [PubMed: 7577575]
13. Hess J, Angel P, Schorpp-Kistner M. AP-1 subunits: quarrel and harmony among siblings. J Cell Sci. 2004; 117 (Pt 25) 5965–73. [PubMed: 15564374]
14. Altieri DC. Survivin, cancer networks and pathway-directed drug discovery. Nat Rev Cancer. 2008; 8 (1) 61–70. [PubMed: 18075512]
15. Murata-Hori M, Tatsuka M, Wang YL. Probing the dynamics and functions of aurora B kinase in living cells during mitosis and cytokinesis. Mol Biol Cell. 2002; 13 (4) 1099–108. DOI: 10.1091/mbc.01-09-0467 [PubMed: 11950924]

16. Dekoninck S, Hannezo E, Sifrim A, Miroshnikova YA, Aragona M, Malfait M, et al. Defining the Design Principles of Skin Epidermis Postnatal Growth. Cell. 2020; 181 (3) 604–20. e22 doi: 10.1016/j.cell.2020.03.015 [PubMed: 32259486]
17. Joost S, Zeisel A, Jacob T, Sun X, La Manno G, Lonnerberg P, et al. Single-Cell Transcriptomics Reveals that Differentiation and Spatial Signatures Shape Epidermal and Hair Follicle Heterogeneity. Cell Syst. 2016; 3 (3) 221–37. e9 doi: 10.1016/j.cels.2016.08.010 [PubMed: 27641957]
18. Joost S, Jacob T, Sun X, Annusver K, La Manno G, Sur I, Kasper M. Single-Cell Transcriptomics of Traced Epidermal and Hair Follicle Stem Cells Reveals Rapid Adaptations during Wound Healing. Cell Rep. 2018; 25 (3) 585–97. e7 [PubMed: 30332640]
19. Bansaccal N, Vieugue P, Sarate R, Song Y, Minguijon E, Miroshnikova YA, et al. The extracellular matrix dictates regional competence for tumour initiation. Nature. 2023; 623 (7988) 828–35. DOI: 10.1038/s41586-023-06740-y [PubMed: 37968399]
20. Sang Y, Kong P, Zhang S, Zhang L, Cao Y, Duan X, et al. SGK1 in Human Cancer: Emerging Roles and Mechanisms. Front Oncol. 2020; 10 608722 doi: 10.3389/fonc.2020.608722 [PubMed: 33542904]
21. Vietri Rudan M, Watt FM. Mammalian Epidermis: A Compendium of Lipid Functionality. Front Physiol. 2021; 12 804824 doi: 10.3389/fphys.2021.804824 [PubMed: 35095565]
22. Talarico C, D'Antona L, Scumaci D, Barone A, Gigliotti F, Fiumara CV, et al. Preclinical model in HCC: the SGK1 kinase inhibitor SI113 blocks tumor progression in vitro and in vivo and synergizes with radiotherapy. Oncotarget. 2015; 6 (35) 37511–25. DOI: 10.18632/oncotarget.5527 [PubMed: 26462020]
23. Enzo E, Secone Seconetti A, Forcato M, Tenedini E, Polito MP, Sala I, et al. Single-keratinocyte transcriptomic analyses identify different clonal types and proliferative potential mediated by FOXM1 in human epidermal stem cells. Nat Commun. 2021; 12 (1) 2505. doi: 10.1038/s41467-021-22779-9 [PubMed: 33947848]
24. Brun SN, Markant SL, Esparza LA, Garcia G, Terry D, Huang JM, et al. Survivin as a therapeutic target in Sonic hedgehog-driven medulloblastoma. Oncogene. 2015; 34 (29) 3770–9. DOI: 10.1038/onc.2014.304 [PubMed: 25241898]
25. Schwitalla S, Fingerle AA, Cammareri P, Nebelsiek T, Goktuna SI, Ziegler PK, et al. Intestinal tumorigenesis initiated by dedifferentiation and acquisition of stem-cell-like properties. Cell. 2013; 152 (1-2) 25–38. [PubMed: 23273993]
26. Vasioukhin V, Degenstein L, Wise B, Fuchs E. The magical touch: genome targeting in epidermal stem cells induced by tamoxifen application to mouse skin. Proc Natl Acad Sci U S A. 1999; 96 (15) 8551–6. DOI: 10.1073/pnas.96.15.8551 [PubMed: 10411913]
27. Nguyen H, Rendl M, Fuchs E. Tcf3 governs stem cell features and represses cell fate determination in skin. Cell. 2006; 127 (1) 171–83. [PubMed: 17018284]
28. Dobin A, Davis CA, Schlesinger F, Drenkow J, Zaleski C, Jha S, et al. STAR: ultrafast universal RNA-seq aligner. Bioinformatics. 2013; 29 (1) 15–21. DOI: 10.1093/bioinformatics/bts635 [PubMed: 23104886]
29. Anders S, Pyl PT, Huber W. HTSeq--a Python framework to work with high-throughput sequencing data. Bioinformatics. 2015; 31 (2) 166–9. DOI: 10.1093/bioinformatics/btu638 [PubMed: 25260700]
30. Zheng GX, Terry JM, Belgrader P, Ryvkin P, Bent ZW, Wilson R, et al. Massively parallel digital transcriptional profiling of single cells. Nat Commun. 2017; 8 14049 doi: 10.1038/ncomms14049 [PubMed: 28091601]
31. Hao Y, Hao S, Andersen-Nissen E, Mauck WM 3rd, Zheng S, Butler A, et al. Integrated analysis of multimodal single-cell data. Cell. 2021; 184 (13) 3573–87. e29 doi: 10.1016/j.cell.2021.04.048 [PubMed: 34062119]
32. Becht E, McInnes L, Healy J, Dutertre CA, Kwok IWH, Ng LG, et al. Dimensionality reduction for visualizing single-cell data using UMAP. Nat Biotechnol. 2019; 37: 38–44. [PubMed: 30531897]

Europe PMC Funders Author Manuscripts

Statement of significance

This study identifies Survivin as key regulator of the different ability of stem cells and progenitors to initiate skin cancer. Survivin expression in oncogene-targeted stem cells is essential for their survival and self-renewal and to prevent their differentiation and apoptosis, allowing stem cells and not progenitors to initiate skin cancer.

Europe PMC Funders Author Manuscripts

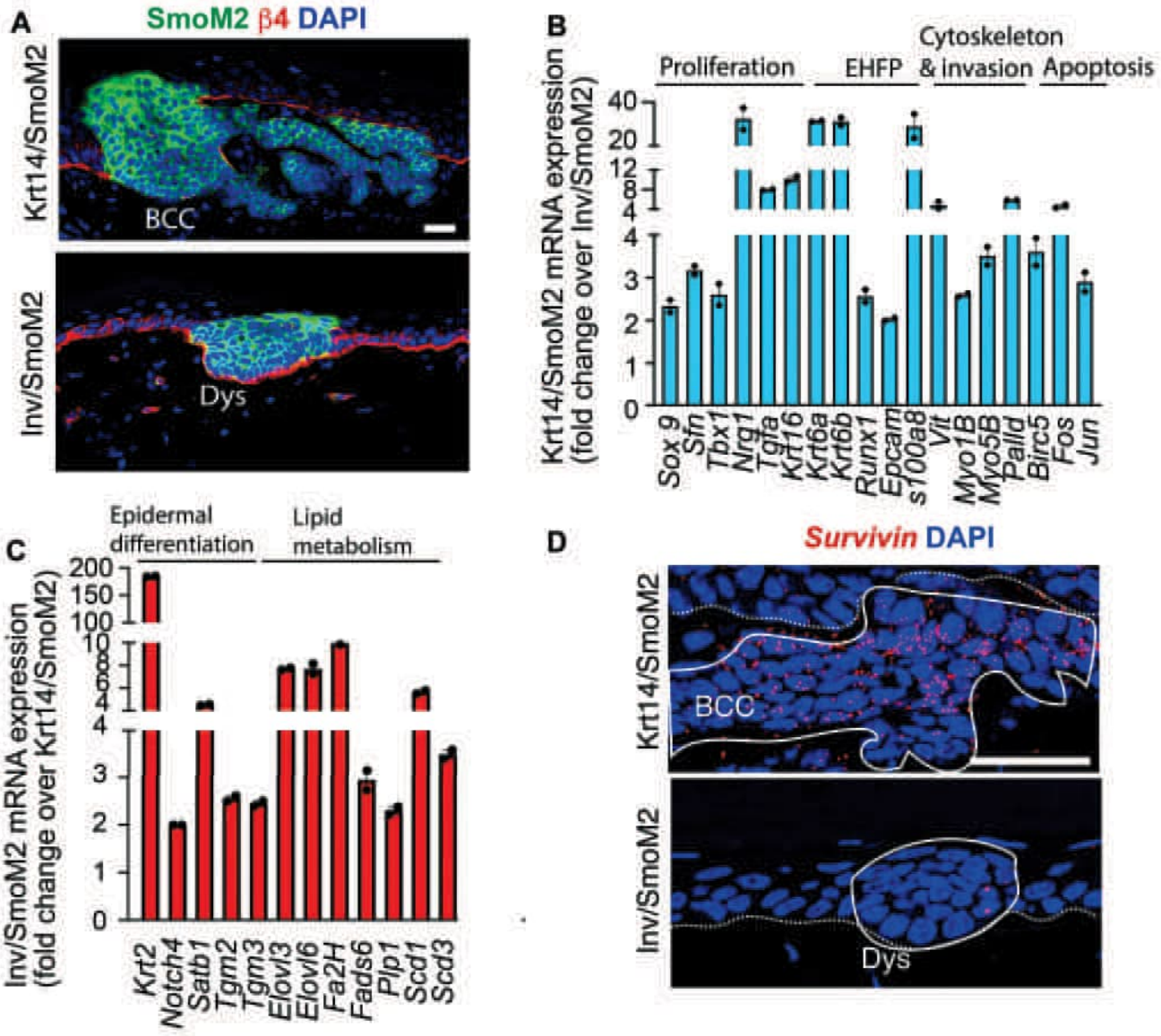

Figure 1. Survivin expression in SCs and P following SmoM2 expression.

A, Image of tail skin section showing immunostaining for β4-integrin and SmoM2 in *Krt14/SmoM2* and *Inv/SmoM2* mice at 8 weeks after tamoxifen administration. **B**, mRNA expression of genes upregulated in SmoM2-expressing SCs as compared to SmoM2-expressing Ps as defined by RNAseq (n=2 mean ± s.e.m). **C**, mRNA expression of genes upregulated in SmoM2-expressing Ps as compared to SmoM2-expressing SCs as defined by RNAseq (n=2 mean ± s.e.m). **D**, RNA FISH for *Birc5/Survivin* in SmoM2-expressing SCs and Ps. Scale bar 20 μm in A,D.

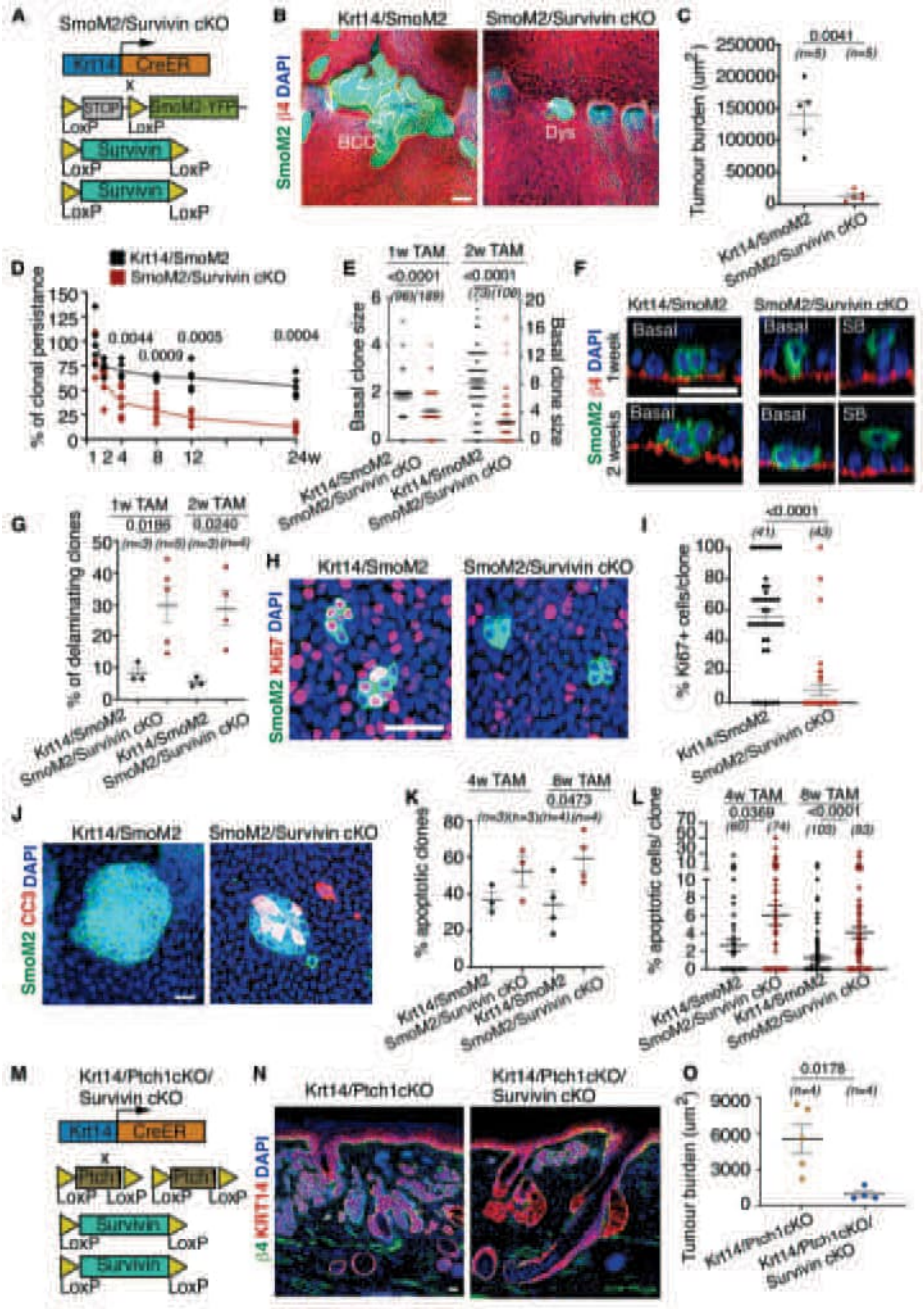

Figure 2. *Survivin* deletion in SCs prevents BCC formation.

A, Genetic strategy to activate *SmoM2* expression and delete *Survivin* in epidermal SCs. **B**, Confocal analysis of immunostaining for SmoM2 and β4-integrin on whole mounts tail skin of *Krt14/SmoM2* and *SmoM2/Survivin cKO* mice at 12 weeks after tamoxifen administration. **C**, Quantification of the tumour burden defined by the area occupied by the SmoM2 tumorigenic lesions in a skin surface area comprised by 6 groups of triplets of hair follicles in *Krt14/SmoM2* and *SmoM2/Survivin cKO* mice 12 weeks after tamoxifen administration (n=mice). Statistical analysis was determined using Welch's t

Europe PMC Funders Author Manuscripts

test **D**, Quantification of the clonal persistence in the interscale region of *Krt14/SmoM2* and *SmoM2/Survivin cKO* mice at different times of tamoxifen administration of at least n= 5 animals per timepoint/genotype. Statistical analysis was determined using two-way ANOVA test. **E**, Basal clone size in *Krt14/SmoM2* and *SmoM2/Survivin cKO* mice at 1 week and 2 weeks after tamoxifen administration. (n=clones quantified from at least 3 different animals). Statistical analysis was determined using Mann-Whitney test. **F**, Confocal analysis of immunostaining for SmoM2 and β4-integrin in *Krt14/SmoM2* and *SmoM2/Survivin cKO* mice at 1 week and 2 weeks after tamoxifen administration. Orthogonal view was used to quantify the number of basal and suprabasal cells per clone. **G**, Percentage of clones presenting only suprabasal cells (delaminating/differentiating clones) in *Krt14/SmoM2* and *SmoM2/Survivin cKO* mice at 1 week and 2 weeks after tamoxifen administration. (n=animals analysed). Statistical significance was assessed using Welch's t test. **H**, Immunostaining for Ki67 and SmoM2 at 2 weeks after tamoxifen administration in *Krt14/SmoM2* and *SmoM2/Survivin cKO* mice. **I**, Percentage of Ki67+ cells per clone at 2 weeks after SmoM2 activation in *Krt14/SmoM2* and *SmoM2/Survivin cKO* mice. (n= clones quantified from 2 different animals). Statistical significance was assessed using Mann-Whitney test. **J**, Immunostaining for Cleaved Caspase3 (CC3) and SmoM2 at 8 weeks after tamoxifen administration in *Krt14/SmoM2* and *SmoM2/Survivin cKO* mice. **K**, Quantification of the number of apoptotic clones at 4 and 8 weeks after SmoM2 activation in *Krt14/SmoM2* and *SmoM2/Survivin cKO* mice. (n=mice). Statistical significance was assessed using Welch's t test. **L**, Quantification of the number of apoptotic cells per clone at 4 and 8 weeks after SmoM2 activation in *Krt14/SmoM2* and *SmoM2/Survivin cKO* mice. (n= clones quantified from at least 3 different animals). Statistical significance was assessed using Mann-Whitney test. **M**, Genetic strategy to delete both *Ptch1* and *Survivin* in SCs. **N**, Image of ventral skin sections showing immunostaining for Krt14 and β4-integrin in *Krt14/Ptch1 cKO* and *Krt14/Ptch1cKO/Survivin cKO* mice at 12 weeks after tamoxifen administration. **O**, Tumour burden in *Krt14/Ptch1cKO* and *Krt14/Ptch1cKO/Survivin cKO* mice. (n=mice). Statistical significance was assessed using Welch's t test. Error bars represent the mean ± s.e.m in each figure. Scale bar 50 μm in B, 20 μm in F, H, J and 20 μm in N.

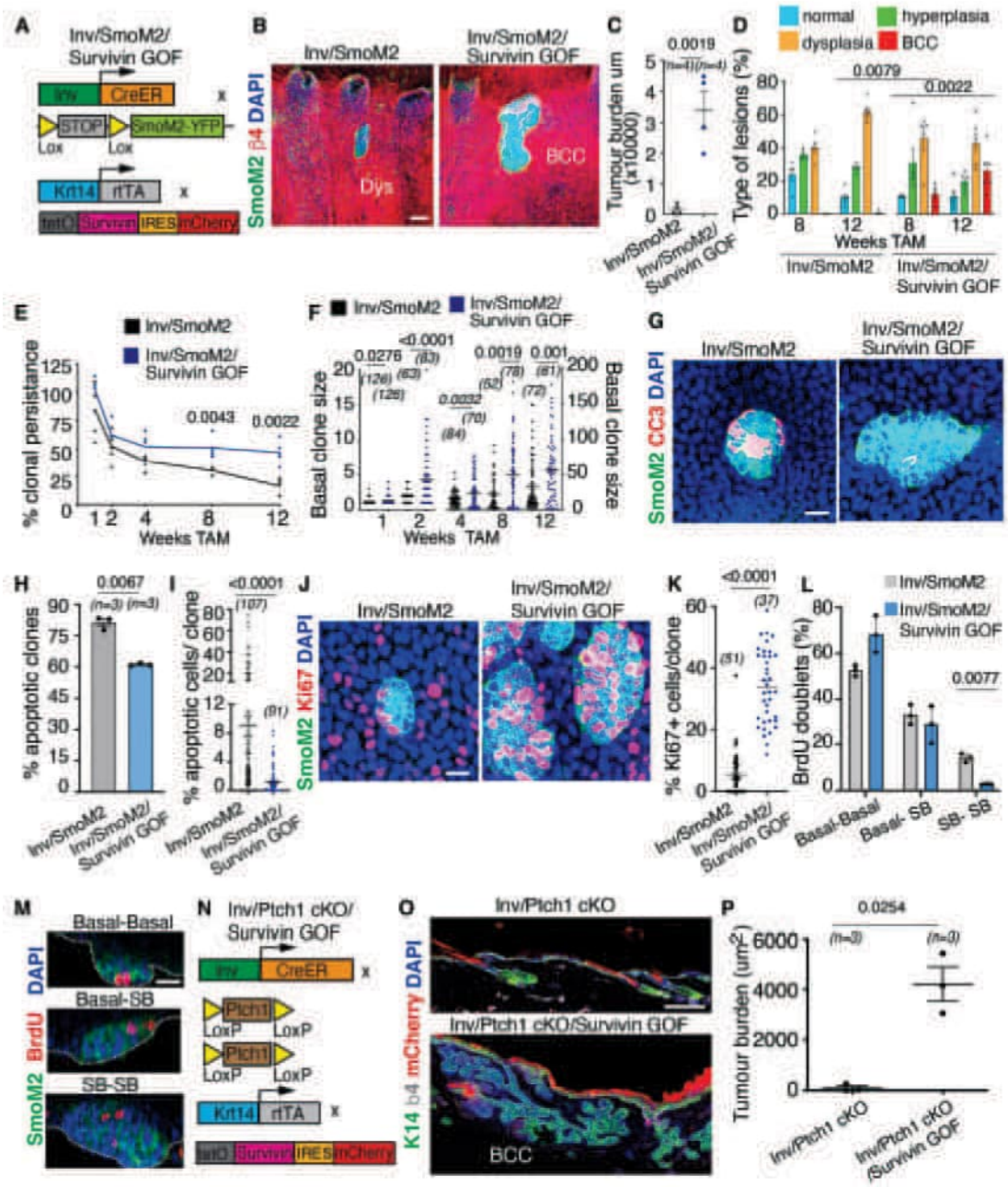

Figure 3. *Survivin* overexpression in Ps confers the competence for BCC initiation.

A, Genetic strategy to activate SmoM2 and overexpress *Survivin* in Ps. **B**, Confocal analysis of immunostaining for SmoM2 and β4-integrin on whole mounts tail skin from *Inv/SmoM2* and *Inv/SmoM2/Survivin GOF* mice at 12 weeks after tamoxifen administration. **C**, Tumour burden in *Inv/SmoM2* and *Inv/SmoM2/Survivin GOF* mice at 12 weeks after tamoxifen administration. (n=mice). Statistical significance was assessed using Mann-Whitney test. **D**, Quantification of the lesion morphology in *Inv/SmoM2* and *Inv/SmoM2/Survivin GOF* mice at 8 and 12 weeks after tamoxifen administration. (n=mice). Statistical significance

was assessed using Mann-Whitney test **E**, Quantification of the clonal persistence in the interscale region of *Inv/SmoM2* and *Inv/SmoM2/Survivin GOF* mice at different times of tamoxifen administration of at least n= 5 animals per timepoint/genotype. Statistical significance was assessed using Mann-Whitney test. **F**, Basal clone sizes in *Inv/SmoM2* and *Inv/SmoM2/Survivin GOF* mice at different times of tamoxifen administration. (n=clones from 2 mice). Statistical significance was assessed using Mann-Whitney test. **G**, Immunostaining for Cleaved Caspase3 (CC3) and SmoM2 at 8 weeks after tamoxifen administration in *Inv/SmoM2* and *Inv/SmoM2/Survivin GOF* mice. **H**, Quantification of the number of apoptotic clones at 8 weeks after tamoxifen administration in *Inv/SmoM2* and *Inv/SmoM2/Survivin GOF* mice. (n = 3 mice). Significance was determined using Welch's t test. **I**, Quantification of the number of apoptotic cells per clone at 8 weeks after tamoxifen administration in *Inv/SmoM2* and *Inv/SmoM2/SurvivinGOF* mice. (n = clones analysed from 3 different animals). Statistical significance was assessed using Mann-Whitney test. **J**, Confocal analysis of immunostaining for SmoM2 and β4-integrin on whole mounts tail skin of *Inv/SmoM2* and *Inv/SmoM2/Survivin GOF* mice at 8 weeks after tamoxifen administration. **K**, Percentage of Ki67+ cells per clone at 2 weeks after SmoM2 activation in *Inv/SmoM2* and *Inv/SmoM2/Survivin GOF* mice. (n = clones from 3 mice). Significance was determined using Mann-Whitney test. **L**, BrdU short term lineage tracing to define cell fate outcome of progenitors (BrdU doublets) in *Inv/SmoM2* and *Inv/SmoM2/Survivin GOF* mice at 8 weeks. (n = 3 mice/group). Statistical significance was assessed using Welch's t test. **M**, Short-term fate outcome of progenitors in Inv/SmoM2/Survivin GOF clones at 8 weeks, as assessed by using BrdU as a clonal marker. Only cell doublets were counted and classified as either basal–basal, basal–suprabasal, or suprabasal–suprabasal. Immunostaining for BrdU and SmoM2 showing the different type of cell fate outcomes found in Inv/SmoM2/ Survivin GOF clones. **N**, Genetic strategy to delete *Ptch1* and overexpress *Survivin* in Ps. **O**, Image of ventral skin sections showing immunostaining for Krt14 and β4-integrin and endogenous expression of mCherry in *Inv/Ptch1 cKO* and *Inv/Ptch1 cKO/Survivin GOF* mice at 12 weeks following tamoxifen administration. **P**, Tumour burden in *Inv/Ptch1 cKO* and *Inv/Ptch1cKO/Survivin GOF* mice at 12 weeks after tamoxifen administration. (n= mice). Statistical significance was assessed using Welch's t test. Error bars represent the mean ± s.e.m in each figure. Scale bar 50 μm in B, 20 μm in G,J,M and 200 μm in O. Number of clones counted in between parentheses.

Europe PMC Funders Author Manuscripts

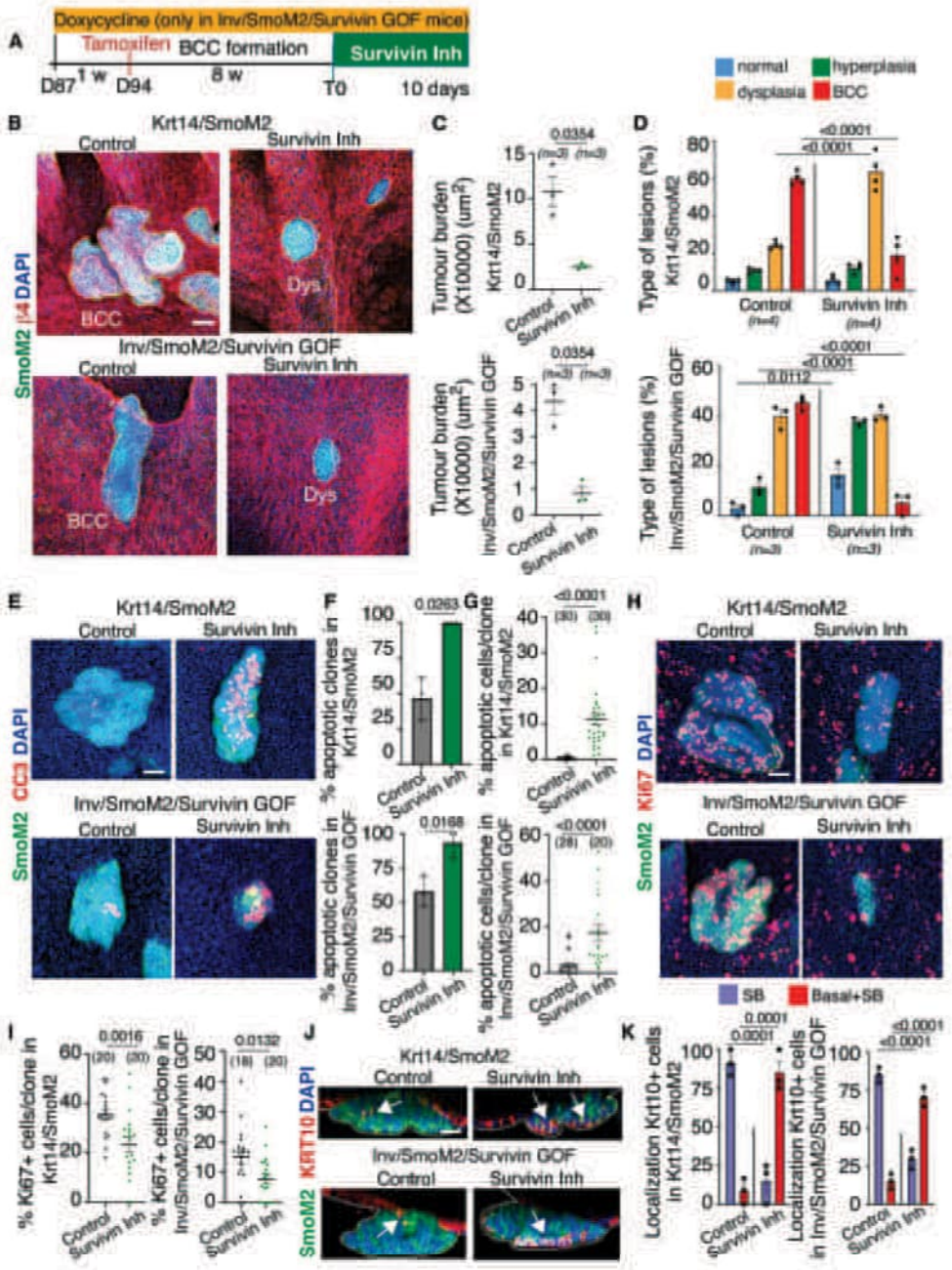

Figure 4. Survivin inhibitor treatment prevents the conversion of preneoplastic lesions into BCCs.

A, Protocol for tumour induction and Survivin inhibitor treatment **B**, Confocal analysis of immunostaining for SmoM2 and β4-integrin on whole mounts tail skin of *Krt14/SmoM2* and *Inv/SmoM2/Survivin GOF* mice at the end of the Survivin inhibitor treatment. **C**, Tumour burden *Krt14/SmoM2* and *Inv/SmoM2/Survivin GOF* mice at the end of the Survivin Inhibitor treatment. (n =mice). Statistical significance was assessed using Mann-Whitney test. **D**, Quantification of the lesion morphology in *Krt14/SmoM2* and *Inv/SmoM2/*

Europe PMC Funders Author Manuscripts

Survivin GOF mice at the end of the Survivin inhibitor treatment and control (n=mice). Statistical significance was assessed using Mann-Whitney test **E**, Immunostaining for CC3 and SmoM2 after Survivin inhibitor treatment in *Krt14/SmoM2* and *Inv/SmoM2/Survivin GOF* mice. **F**, Quantification of the number of apoptotic clones at the end of the Survivin inhibitor treatment in *Krt14/SmoM2* and *Inv/SmoM2/Survivin GOF* mice. (n = 3 mice/group) Significance was determined using Welch's t test. **G**, Quantification of the number of apoptotic cells per clone at the end of the Survivin inhibitor treatment in *Krt14/SmoM2* and *Inv/SmoM2/SurvivinGOF* mice. (n = clones analysed from 3 and 2 different animals in *Krt14/SmoM2 Inv/SmoM2/SurvivinGOF* respectively). Statistical significance was assessed using Mann-Whitney test. **H**, Confocal analysis of immunostaining for SmoM2 and Ki67 on whole mounts tail skin of *Krt14/SmoM2* and *Inv/SmoM2/Survivin GOF* mice at the end of the Survivin inhibitor treatment. **I**, Percentage of Ki67+ cells per clone at the end of the Survivin inhibitor treatment in *Krt14/SmoM2* and *Inv/SmoM2/Survivin GOF* mice. (n = clones from 2 mice). Significance was determined using Mann-Whitney test. **J**, Immunostaining for SmoM2 and KRT10 in Krt14/SmoM2 and Inv/SmoM2/Survivin GOF lesions at the end of the Survivin Inhibitor treatment. **K**, Quantification of the tumorigenic lesions from Krt14/SmoM2 and Inv/SmoM2/Survivin GOF mice containing KRT10 in Suprabasal (SB) or Basal+SB layers (n= 3 mice/group). Error bars represent the mean ± s.e.m in each figure. Scale bar 50 μm in B, 20 μm in E,H, J. Number of clones counted in between parentheses.

Europe PMC Funders Author Manuscripts

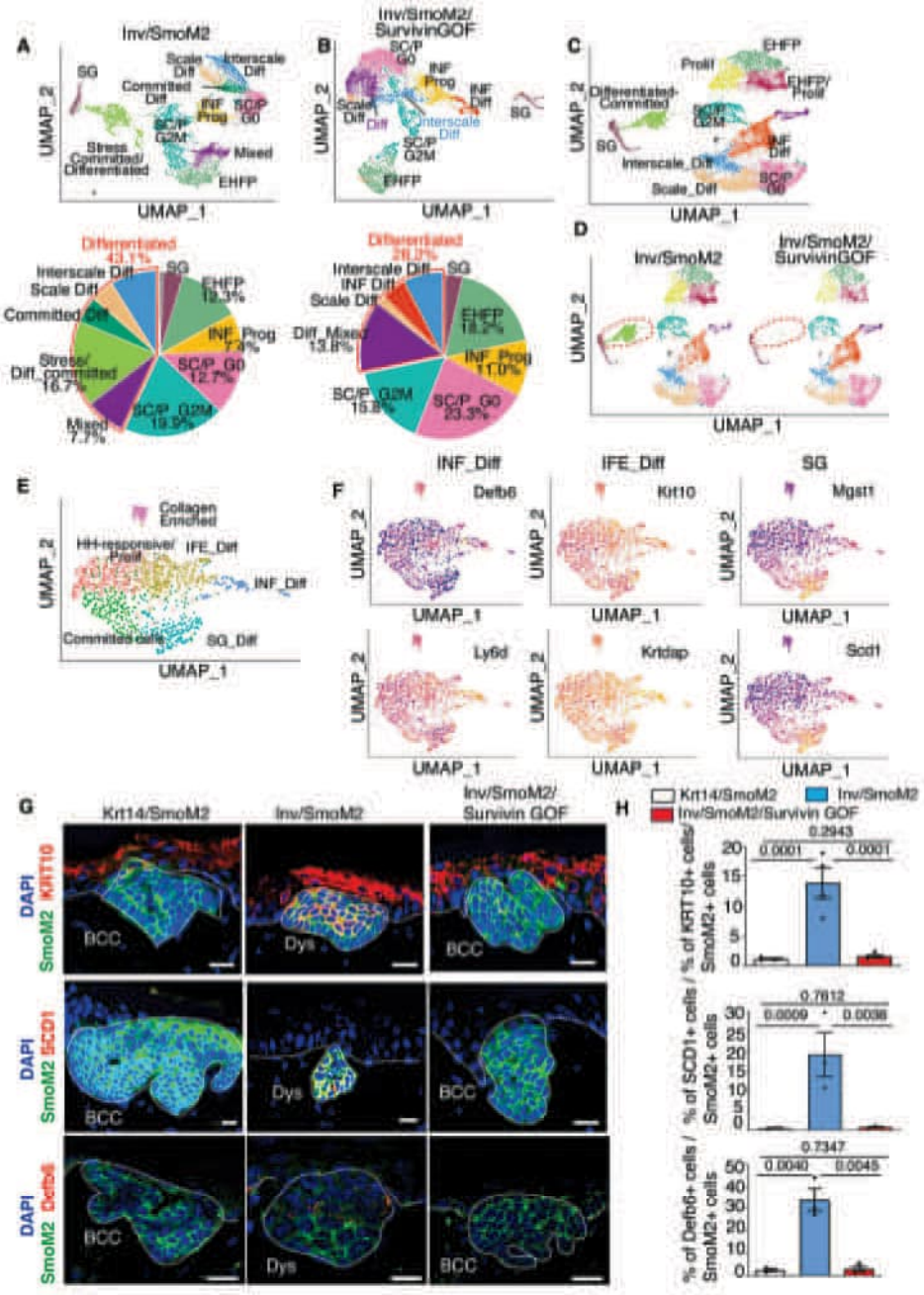

Figure 5. scRNA-seq shows the role of Survivin in preventing keratinocyte differentiation.

A, B Uniform Manifold Approximation and Projection (UMAP) of SmoM2 expressing cells isolated from *Inv/SmoM2* mice (A) and *Inv/SmoM2/SurvivinGOF* mice (B) at 8 weeks after tamoxifen administration showing the different cell type and cell states (upper panel) and their relative proportion (lower panel). **C**, UMAP dimensionality reduction plots representing unsupervised clustering: Integrated data (*Inv/SmoM2* and *Inv/SmoM2/SurvivinGOF*) using Seurat **D**, UMAP visualization of SmoM2-expressing cells isolated from *Inv/SmoM2* mice and *Inv/SmoM2/SurvivinGOF* mice after data integration **E**,

Subclustering of the Differentiated/Committed cluster of the *Inv/SmoM2* integrated data is no longer present following Survivin overexpression. **F**, Cell states found following subclustering of the Differentiated/Committed cluster found in *Inv/SmoM2* integrated data. Colour code by normalized gene expression for specific genes for Interfollicular epidermis progenitor (*Krt10* and *Krtdap*), Infundibulum differentiation (*Defb6* and *Ly6d*), and Sebaceous gland (*Mgst1* and *Scd1*). **G**, Immunostaining for SmoM2-GFP, Keratin10 (K10) and SCD1, and *in situ* hybridization for Defb6 in *Krt14/SmoM2, Inv/SmoM2/SurvivinGOF* and *Inv/SmoM2* mice at 8 weeks after tamoxifen administration, **H**, Quantification of immunostaining for $KRT10^+$ cells, $SCD1^+$ cells and $Defb6^+$ cells in SmoM2-expressing clones from *Krt14/SmoM2, Inv/SmoM2/SurvivinGOF* and *Inv/SmoM2* mice at 8 weeks after tamoxifen administration (n=3 animals/genotype). Significance was determined using Mann-Whitney test. Error bars represent the mean ± s.e.m in each figure. Scale bar 20 μm in G.

Europe PMC Funders Author Manuscripts

Europe PMC Funders Author Manuscripts

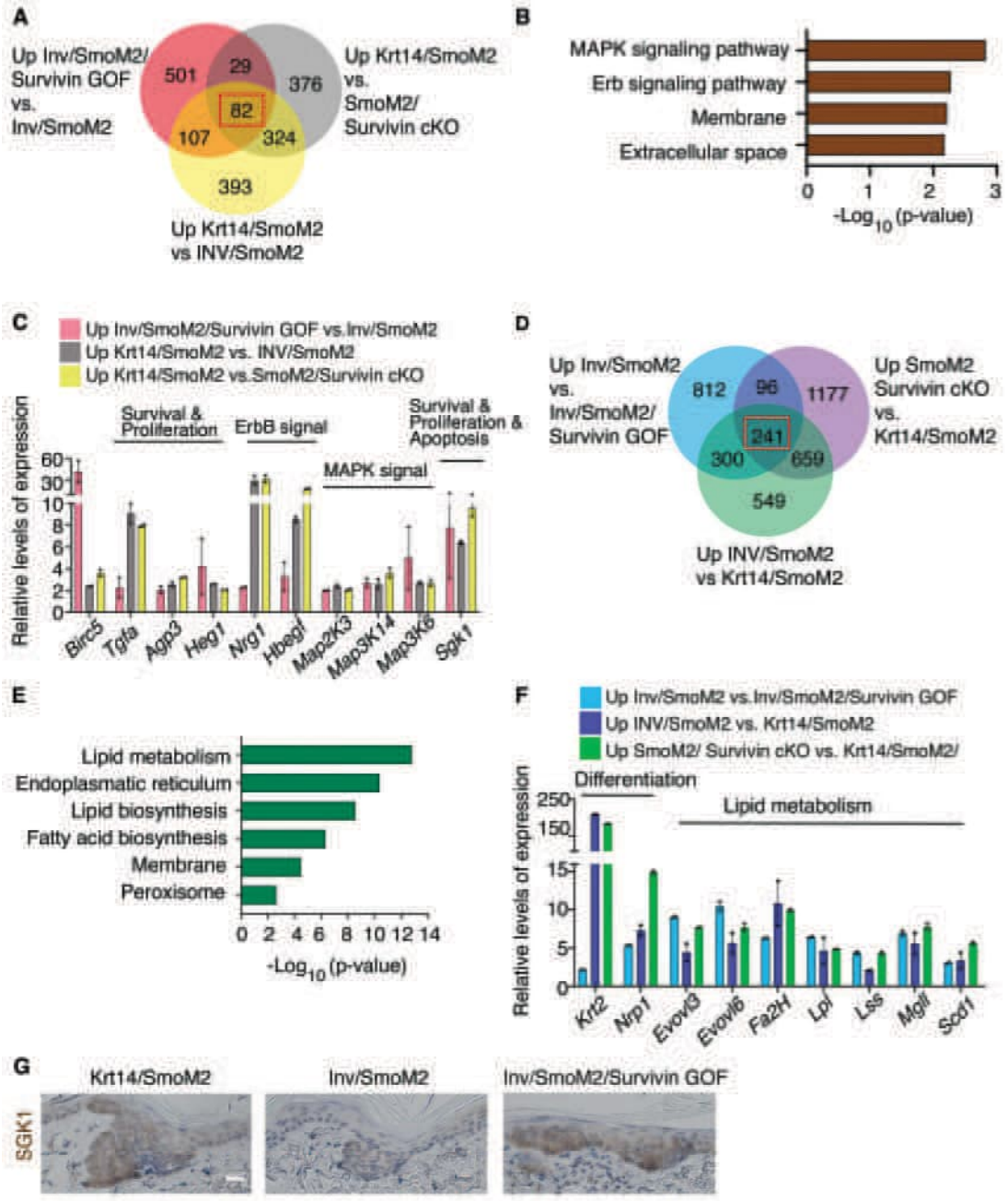

Figure 6. *Survivin* promotes proliferation and survival and prevents apoptosis and keratinocyte differentiation in SmoM2-expressing cells.

A, Venn diagram showing the common genes upregulated following *Survivin* expression in 3 different conditions: up *Krt14/SmoM2* vs *Inv/SmoM2* 8 weeks upon tamoxifen administration (yellow colour), up *Inv/SmoM2/Surivivin GOF* vs *Inv/SmoM2* 8 weeks upon tamoxifen administration (pink colour) and up *Krt14/SmoM2* vs *SmoM2/Survivin cKO* 6 weeks upon tamoxifen administration (grey colour). **B**, Gene ontology (GO) analysis of 82 genes upregulated in the 3 conditions analysed. **C**, Relative mRNA expression of the genes

upregulated in the 3 conditions analysed as defined by RNAseq (n=2 mean ± s.e.m). **D**, Venn diagram showing the genes commonly downregulated following *Survivin* expression in 3 different conditions: up *Inv14/SmoM2* vs *Krt14/SmoM2* 8 weeks after tamoxifen administration (green colour), up *Inv/SmoM2* vs *Inv/SmoM2/SurvivinGOF* 8 weeks after tamoxifen administration (blue colour) and up *SmoM2/Survivin cKO* vs *Krt14/SmoM2* 6 weeks after tamoxifen (purple colour) **E**, GO analysis of 241 genes downregulated in the 3 conditions analysed. **F**, Relative mRNA expression of the genes upregulated in the 3 conditions analysed as defined by RNAseq (n=2 mean ± s.e.m). **G**, SGK1 immunohistochemistry of tail skin sections in *Krt14/SmoM2, Inv/SmoM2* and *Inv/SmoM2/Survivin GOF* mice at 8 weeks after tamoxifen administration.

Europe PMC Funders Author Manuscripts

Europe PMC Funders Author Manuscripts

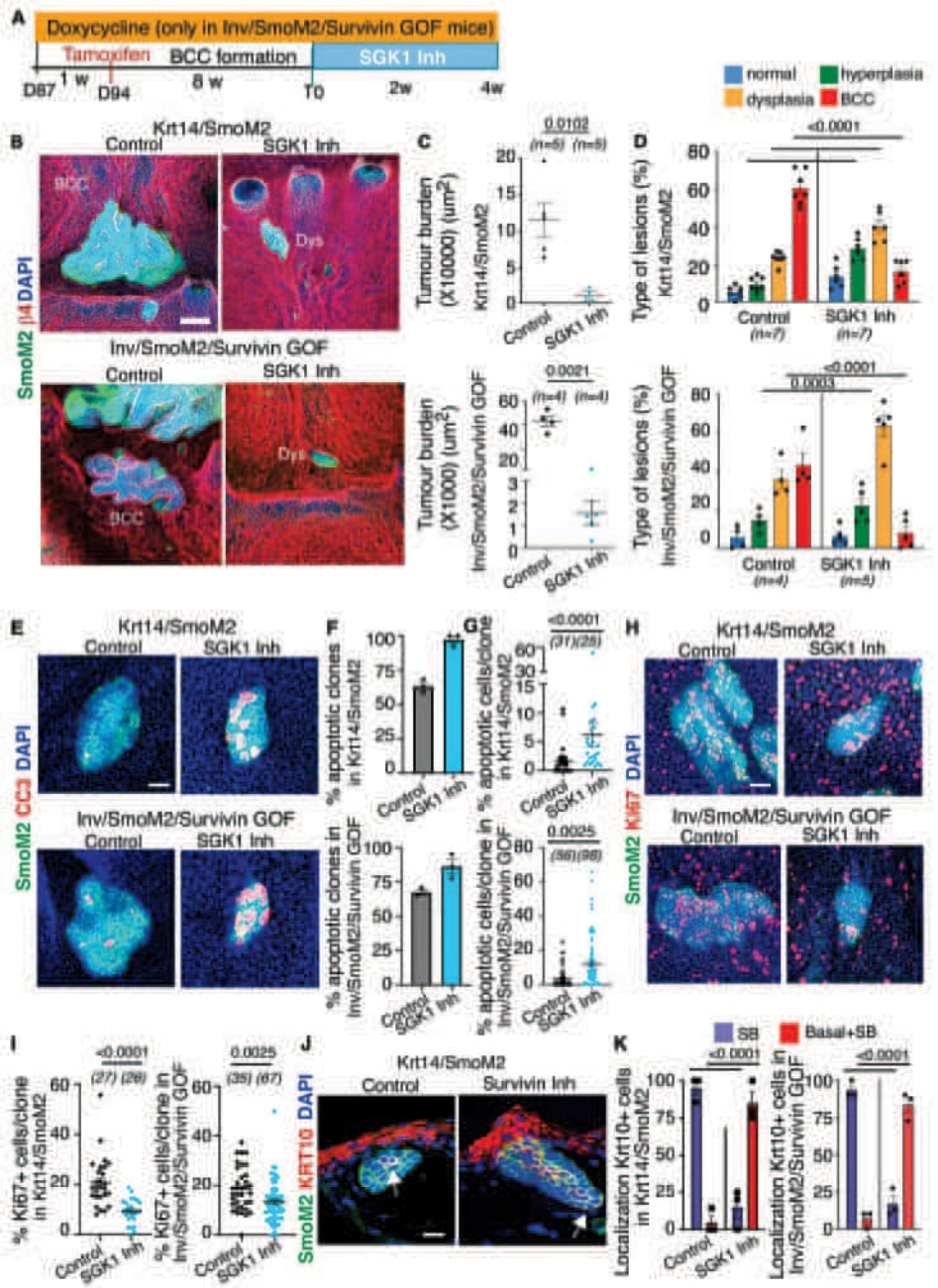

Figure 7. SGK 1 inhibition prevents BCC formation in Survivin-expressing cells.

A, Protocol used for the treatment of *Krt14/SmoM2* and *Inv/SmoM2/Survivin GOF* mice with SGK1 inhibitor. **B**, Confocal analysis of immunostaining for SmoM2 and β4-integrin on whole mounts tail skin of *Krt14/SmoM2 and Inv/SmoM2/Survivin GOF* mice treated 4 weeks with SGK 1 inhibitor and control mice. **C**, Tumour burden in *Krt14/SmoM2 and Inv/SmoM2/Survivin GOF* mice treated for 4 weeks with SGK 1 inhibitor and control mice. (n = mice). Statistical significance was assessed using Welch's t test. **D**, Quantification of the types of lesions in *Krt14/SmoM2 and Inv/SmoM2/Survivin GOF* mice treated for

Europe PMC Funders Author Manuscripts

4 weeks with SGK1 inhibitor and control mice. (n = mice). Statistical significance was assessed using two-way ANOVA with Sidak's multiple comparison test. **E**, Immunostaining for CC3 and SmoM2 after SGK1 inhibitor treatment in *Krt14/SmoM2* and *Inv/SmoM2/Survivin GOF* mice. **F**, Quantification of the number of apoptotic clones at 2 weeks of SGK1 inhibitor treatment in *Krt14/SmoM2* and *Inv/SmoM2/Survivin GOF* mice. (n=3 mice/group). Significance was determined using Welch's t test. **G**, Quantification of the number of apoptotic cells per clone at 2 weeks of SGK1 inhibitor treatment in *Krt14/SmoM2* and *Inv/SmoM2/Survivin GOF* mice. (n = clones from 3 and 2 mice *Krt14/SmoM2* and *Inv/SmoM2/Survivin GOF* mice respectively). Statistical significance was assessed using Mann-Whitney test. **H**, Confocal analysis of immunostaining for SmoM2 and Ki67 on whole mounts tail skin of *Krt14/SmoM2* and *Inv/SmoM2/Survivin GOF* mice at 2 weeks of the SGK1 inhibitor treatment. **I**, Percentage of Ki67+ cells per clone at 2 weeks of Survivin inhibitor treatment in *Krt14/SmoM2* and *Inv/SmoM2/Survivin GOF* mice. (n = clones from 3 mice). Significance was determined using Mann-Whitney test. **J**, Immunostaining for SmoM2 and KRT10 in sections in *Krt14/SmoM2* lesions at 2 weeks of SGK1 Inhibitor treatment. **K**, Quantification of the tumorigenic lesions from *Krt14/SmoM2* and *Inv/SmoM2/Survivin GOF* mice containing KRT10 in Suprabasal (SB) or Basal+SB layers at 2 weeks of SGK1 inhibitor treatment. (n=3 mice/group). Statistical analysis was determined using two-way ANOVA test. Error bars represent the mean ± s.e.m in each figure. Scale bar 50 μm in B, 20 μm in E,H, J. Number of clones counted in between parentheses.

Tetracycline response element- bglobin intron- cDNA Birc5- IRES- mCherry

1 CTCGAGTTTA CTCCCTATCA GTGATAGAGA ACGTATGTCG AGTTTACTCC CTATCAGTGA
61 TAGAGAACGA TGTCGAGTTT ACTCCCTATC AGTGATAGAG AACGTATGTC GAGTTTACTC
121 CCTATCAGTG ATAGAGAACG TATGTCGAGT TTACTCCCTA TCAGTGATAG AGAACGTATG
181 TCGAGTTTAT CCCTATCAGT GATAGAGAAC GTATGTCGAG TTTACTCCCT ATCAGTGATA
241 GAGAACGTAT GTCGAGGTAG GCGTGTACGG TGGGAGGCCT ATATAAGCAG AGCTCGTTTA
301 GTGAACCGTC AGATCGCCTG GAGAATTCTG CAGGTGAGTT TGGGGACCCT TGATTGTTCT
361 TTCTTTTTCG CTATTGTAAA ATTCATGTTA TATGGAGGGG GCAAAGTTTT CAGGGTGTTG
421 TTTAGAATGG GAAGATGTCC CTTGTATCAC CATGGACCCT CATGATAATT TTGTTTCTTT
481 CACTTTCTAC TCTGTTGACA ACCATTGTCT CCTCTTATTT TCTTTTCATT TTCTGTAACT
541 TTTTCGTTAA ACTTTAGCTT GCATTTGTAA CGAATTTTTA AATTCACTTT TGTTTATTTG
601 TCAGATTGTA AGTACTTTCT CTAATCACTT TTTTTTCAAG GCAATCAGGG TATATTATAT
661 TGTACTTCAG CACAGTTTTA GAGAACAATT GTTATAATTA AATGATAAGG TAGAATATTT
721 CTGCATATAA ATTCTGGCTG GCGTGGAAAT ATTCTTATTG GTAGAAACAA CTACATCCTG
781 GTCATCATCC TGCCTTTCTC TTTATGGTTA CAATGATATA CACTGTTTGA GATGAGGATA
841 AAATACTCTG AGTCCAAACC GGGCCCCTCT GCTAACCATG TTCATGCCTT CTTCTTTTTC
901 CTACAGGCTA GCCACCATGG GAGCTCCGGC GCTGCCCCAG ATCTGGCAGC TGTACCTCAA
961 GAACTACCGC ATCGCCACCT TCAAGAACTG GCCCTTCCTG GAGGACTGCG CCTGCACCCC
1021 AGAGCGAATG GCGGAGGCTG GCTTCATCCA CTGCCCTACC GAGAACGAGC CTGATTTGGC
1081 CCAGTGTTTT TTCTGCTTTA AGGAATTGGA AGGCTGGGAA CCCGATGACA ACCCGATAGA
1141 GGAGCATAGA AAGCACTCCC CTGGCTGCGC CTTCCTCACT GTCAAGAAGC AGATGGAAGA
1201 ACTAACCGTC AGTGAATTCT TGAAACTGGA CAGACAGAGA GCCAAGAACA AAATTGCAAA
1261 GGAGACCAAC AACAAGCAAA AAGAGTTTGA AGAGACTGCA AAGACTACCC GTCAGTCAAT
1321 TGAGCAGCTG GCTGCCTAAT GACCGCGGGC CCGGGATCCG CCCCTCTCCC TCCCCCCCCC
1381 CTAACGTTAC TGGCCGAAGC CGCTTGGAAT AAGGCCGGTG TGCGTTTGTC TATATGTTAT
1441 TTTCCACCAT ATTGCCGTCT TTTGGCAATG TGAGGGCCCG GAAACCTGGC CCTGTCTTCT
1501 TGACGAGCAT TCCTAGGGGT CTTTCCCCTC TCGCCAAAGG AATGCAAGGT CTGTTGAATG
1561 TCGTGAAGGA AGCAGTTCCT CTGGAAGCTT CTTGAAGACA AACAACGTCT GTAGCGACCC
1621 TTTGCAGGCA GCGGAACCCC CCACCTGGCG ACAGGTGCCT CTGCGGCCAA AAGCCACGTG
1681 TATAAGATAC ACCTGCAAAG GCGGCACAAC CCCAGTGCCA CGTTGTGAGT TGGATAGTTG
1741 TGGAAAGAGT CAAATGGCTC TCCTCAAGCG TATTCAACAA GGGGCTGAAG GATGCCCAGA
1801 AGGTACCCCA TTGTATGGGA TCTGATCTGG GGCCTCGGTA CACATGCTTT ACATGTGTTT
1861 AGTCGAGGTT AAAAAAACGT CTAGGCCCCC CGAACCACGG GGACGTGGTT TTCCTTTGAA
1921 AAACACGATG ATAATATGGC CACAACCATG GTGAGCAAGG GCGAGGAGGA TAACATGGCC
1981 ATCATCAAGG AGTTCATGCG CTTCAAGGTG CACATGGAGG GCTCCGTGAA CGGCCACGAG
2041 TTCGAGATCG AGGGCGAGGG CGAGGGCCGC CCCTACGAGG GCACCCAGAC CGCCAAGCTG
2101 AAGGTGACCA AGGGTGGCCC CCTGCCCTTC GCCTGGGACA TCCTGTCCCC TCAGTTCATG
2161 TACGGCTCCA AGGCCTACGT GAAGCACCCC GCCGACATCC CCGACTACTT GAAGCTGTCC
2221 TTCCCCGAGG GCTTCAAGTG GGAGCGCGTG ATGAACTTCG AGGACGGCGG CGTGGTGACC
2281 GTGACCCAGG ACTCCTCCCT GCAGGACGGC GAGTTCATCT ACAAGGTGAA GCTGCGCGGC
2341 ACCAACTTCC CCTCCGACGG CCCCGTAATG CAGAAGAAGA CCATGGGCTG GGAGGCCTCC
2401 TCCGAGCGGA TGTACCCCGA GGACGGCGCC CTGAAGGGCG AGATCAAGCA GAGGCTGAAG
2461 CTGAAGGACG GCGGCCACTA CGACGCTGAG GTCAAGACCA CCTACAAGGC CAAGAAGCCC
2521 GTGCAGCTGC CCGGCGCCTA CAACGTCAAC ATCAAGTTGG ACATCACCTC CCACAACGAG
2581 GACTACACCA TCGTGGAACA GTACGAACGC GCCGAGGGCC GCCACTCCAC CGGCGGCATG
2641 GACGAGCTGT ACAAGTAATG AGCGGCCGCA TCGATAAGCT TGTCGACGAT ATCTCTAGAG
2701 GATCATAATC AGCCATACCA CATTTGTAGA GGTTTTACTT GCTTTAAAAA ACCTCCCACA
2761 CCTCCCCCTG AACCTGAAAC ATAAAATGAA TGCAATTGTT GTTGTTAACT TGTTTATTGC
2821 AGCTTATAAT GGTTACAAAT AAAGCAATAG CATCACAAAT TTCACAAATA AAGCATTTTT
2881 TTCACTGCCT CGAGCTTCCT CGCTCACTGA CTCGCTGCGC TCGGTCGTTC GGCTGCGGCG
2941 AGCGGTATCA GCTCACTCAA AGGCGGTAAT ACGGTTATCC ACAGAATCAG GGGATAACGC
3001 AGGAAAGAAC ATGTGAGCAA AAGGCCAGCA AAAGGCCAGG AACCGTAAAA AGGCCGCGTT

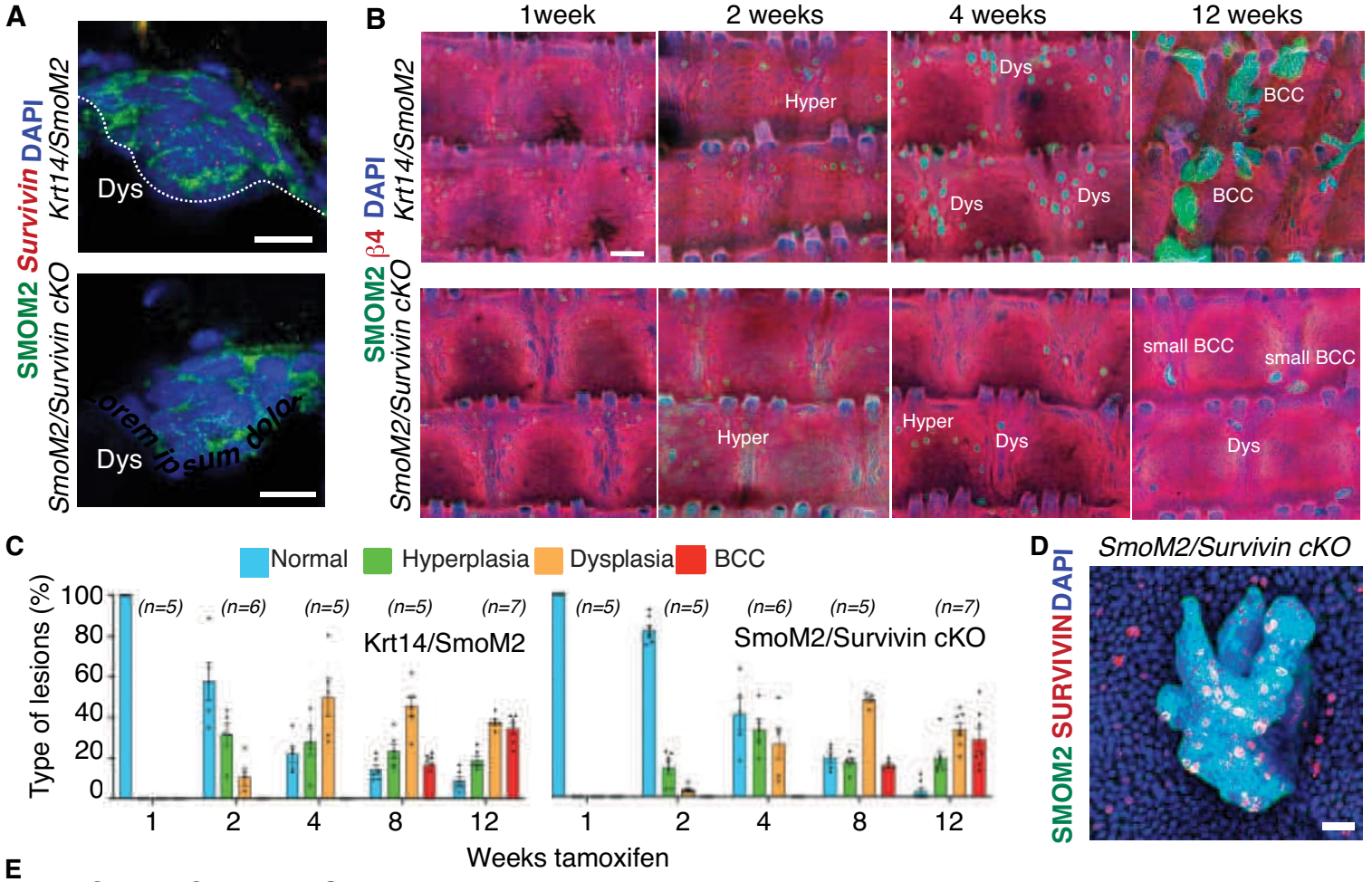

Canato et al, Supplementary Figure S1

Supplementary Fig. S1 –*Survivin* deletion prevents BCC formation. A, *In situ* hybridization for *Birc5/Survivin* in a BCC from *Krt14/SmoM2* and *SmoM2/Survivin cKO* mice at 4 weeks after tamoxifen administration. **B,** Image of whole mount tail skin showing immunostaining for SMOM2 and β4-integrin in *Krt14/SmoM2* and *SmoM2/Survivin cKO* mice at different times of tamoxifen administration. **C**, Quantification of the clone morphology in *Krt14/SmoM2* and *SmoM2/Survivin cKO* mice at different times of tamoxifen administration. (n =number of mice). **D,** Immunostaining for SURVIVIN and SMOM2 in a BCC at 12 weeks upon tamoxifen in *SmoM2/Survivin cKO***. E**, *In situ* hybridization for *Birc5* (left panels), positive control probe (middle panel) and negative control probe (right panel) in BCCs from *SmoM2/Survivin cKO* mice at 12 weeks after tamoxifen administration. **F**, Immunostaining for SMOM2 and KRT10 in lesions from *Krt14/SmoM2* and *SmoM2/Survivin cKO* mice. **G**, Quantification of the proportion of KRT10+ cells within the lesions from *Krt14/SmoM2* and *SmoM2/Survivin cKO* mice (n=mice). Statistical analysis was determined using Mann-Whitney test.**H**, Immunostaining for SMOM2, KRT10 and SURVIVIN in lesions from *Krt14/SmoM2* mice. **I**, Immunostaining for SMOM2, Aurora Kinase B (AKB) and SURVIVIN in lesions from *Krt14/SmoM2* mice. **J**, Immunostaining for SMOM2, CC3 and SURVIVIN in lesions from *Krt14/SmoM2* mice. Error bars represent the mean ± s.e.m in each figure. Scale bar 200 μm in B and 20 μm in A,D, E,F,H, I and J.

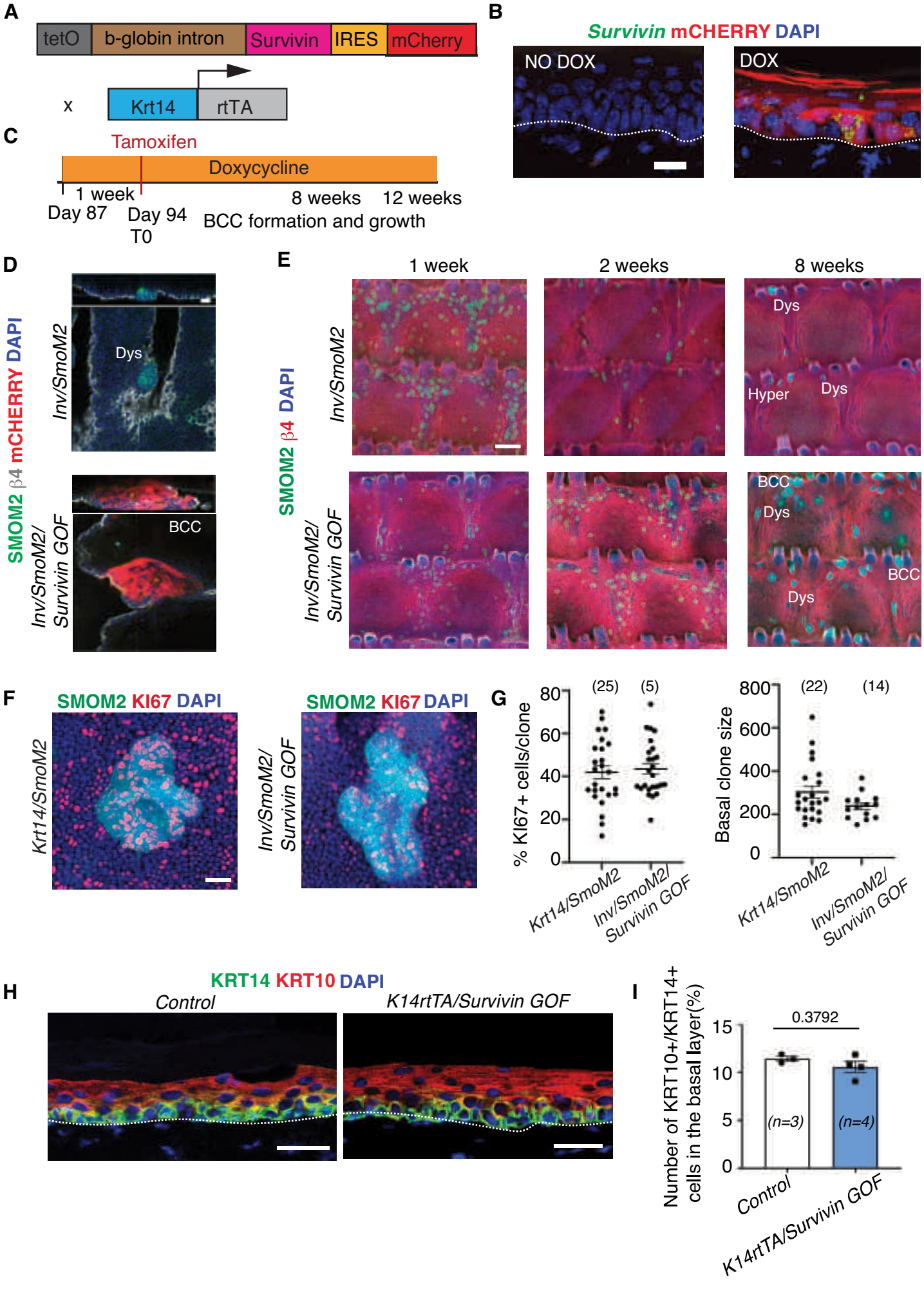

Canato et al, Supplementary Figure S2

Supplementary Fig. S2 - Generation of transgenic mice allowing *Survivin* overexpression in the epidermis. A, Construct used to generate transgenic mice allowing to overexpress *Survivin* together with the mCherry reporter using a doxycycline inducible approach. **B**, Image of skin section from a *K14rtta/TetO-Survivin-IRES-mCherry* mice showing endogenous mCHERRY expression and *Survivin* (*in situ* hybridization) upon doxycycline administration. IRES (internal ribosome entry site). **C**, Protocol used to induce expression of *Survivin* (doxycycline administration) and tumor induction (tamoxifen administration). **D,** Orthogonal projections showing immunostaining for SMOM2 and β4-integrin and endogenous expression of mCHERRY in tail skin of *Inv/SmoM2* and *Inv/SmoM2/Survivin GOF* mice at 12 weeks after tamoxifen administration. **E**, Image of whole mount showing immunostaining for SMOM2 and β4-integrin in *Inv/SmoM2* and *Inv/SmoM2/Survivin GOF* mice at different time points. **F**, Immunostaining for the proliferative marker (KI67) in BCCs derived from *Inv/SmoM2/SurvivinGOF* animals. **G**, Quantification of the number of KI67-positive cells and basal clone size in BCCs derived from *Inv/SmoM2/Survivin GOF*. (Clones counted from 2 different mice/genotype). Statistical analysis was determined using Mann-Whitney test. **H**, Immunostaining for SMOM2 and the basal marker (KRT14), differentiation marker (KRT10) in wild-type skin and skin from *Krt14rtta/Survivin GOF* mice. **I**, Quantification of the number of KRT10 within the basal layer (KRT 14+) in wild type skin and *Krt14rtta/Survivin GOF* mice. Scale bar 20 μm in B, D, F and H and 200 μm in E. Number of clones counted in between parentheses.

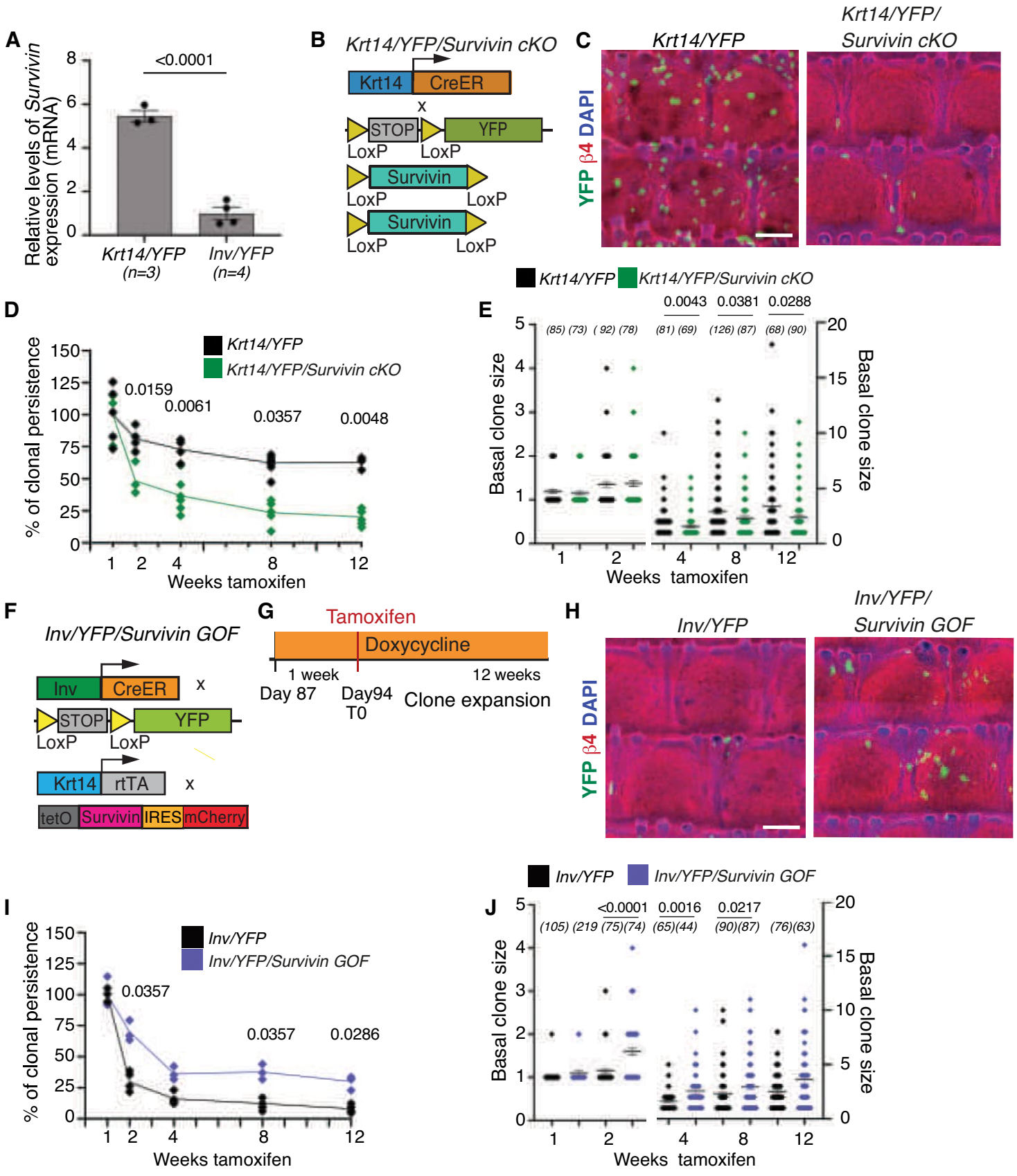

Canato et al, Supplementary Figure S3

Supplementary Fig. S3 – Survivin promotes stem cell-like properties during skin homeostasis. A, Relative levels of expression of *Survivin* in *Krt14/YFP* and *Inv/YFP* clones (n=number of mice). Statistical analysis was determined using Welch's t test. **B**, Genetic approach used to delete *Survivin* together with YFP expression in SCs using the *Krt14CREER*. **C**, Image of whole mount showing immunostaining for YFP and β4-integrin in *Krt14/YFP and Krt14/YFP/Survivin cKO* mice 12 weeks following tamoxifen administration. **D,** Quantification of the clonal persistence in the interscale region of *Krt14/YFP* and *Krt14/YFP/Survivin cKO* mice at different times of tamoxifen administration. (n= minimum 4 mice/group). Statistical analysis was determined using two-way ANOVA test. **E**, Basal clone size in *Krt14/YFP* and *Krt14/YFP/Survivin cKO* mice at different timepoints following tamoxifen administration (n=clones from at least 2 mice). Statistical analysis was determined using Mann-Whitney test. **F**, Genetic approach used to overexpress *Survivin* and YFP in the Inv-progenitors. **G**, Genetic approach used to overexpress *Survivin* using doxycycline administration and induce YFP expression in Ps using *Inv/Rosa-YFP* mice. **H**, Whole mount immunostaining for YFP and β4-integrin in *Inv/YFP and Inv/YFP/Survivin GOF* mice 12 weeks following tamoxifen administration. **I,** Quantification of the clonal persistence in the interscale region of *Inv/YFP* and *Inv/YFP/Survivin GOF* mice at different times of tamoxifen administration. (n= minimum 3 mice/group). Statistical analysis was determined using two-way ANOVA test. **J**, Basal clone size in *Inv/YFP* and *Inv/YFP/Survivin GOF* mice at different timepoints following tamoxifen administration (n=clones from at least 2 mice). Statistical analysis was determined using Mann-Whitney test. Scale bar 20 μm in C and H.

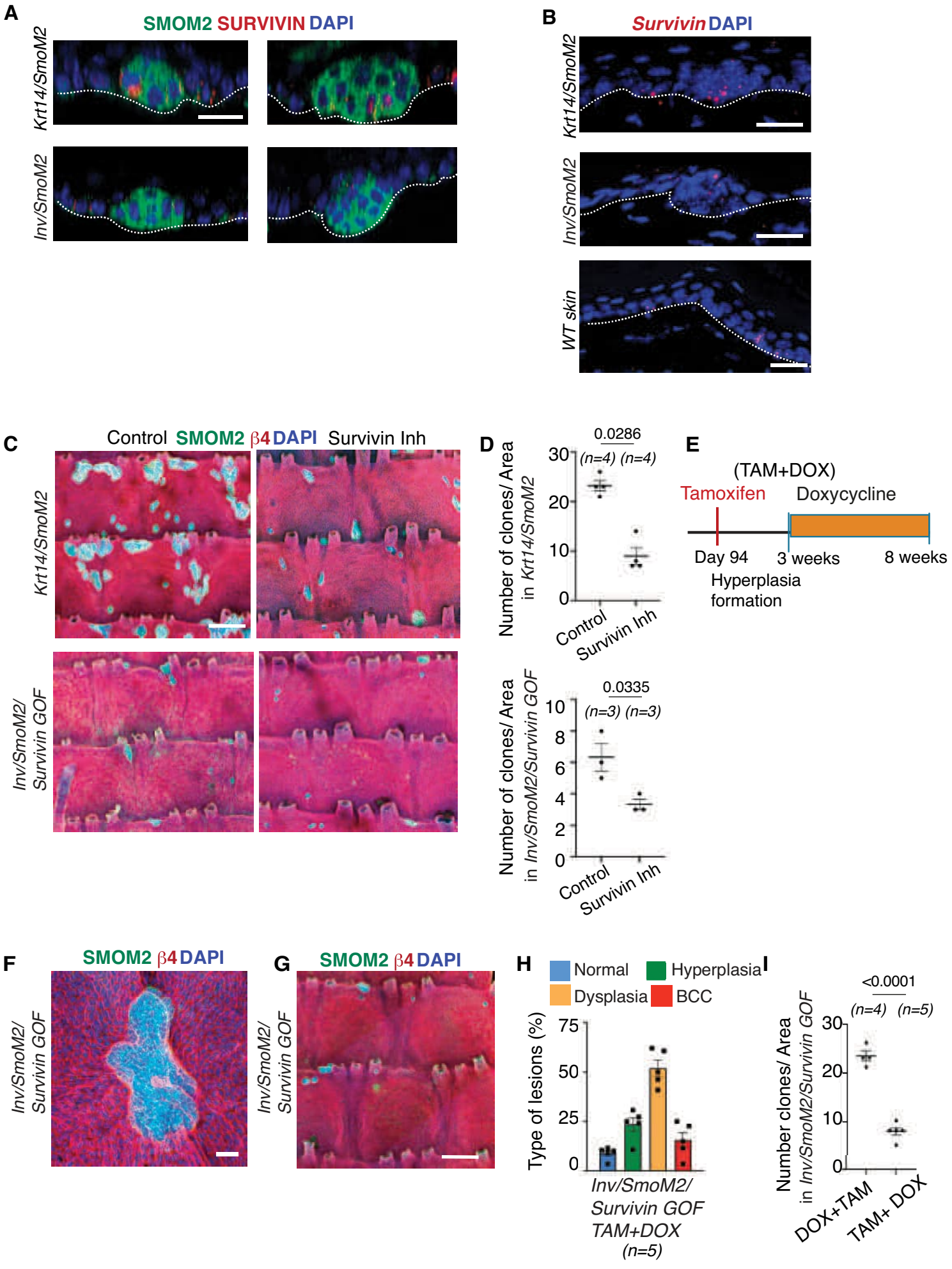

Canato et al, Supplementary Figure S4

Supplementary Fig. S4 – Survivin is expressed in SC derived preneoplastic lesions and Survivin inhibition decreases BCC formation. A, B, Immunostaining for SURVIVIN and SMOM2 (**A**) and *In situ* hybridization for *Survivin* and immunostaining for SMOM2 (**B**) in preneoplastic lesions from *Krt14/SmoM2* and *Inv/SmoM2* mice upon 2 and 4 weeks of tamoxifen administration respectively. **C**, Confocal analysis of whole mount immunostaining for SMOM2 and β4-integrin in *Krt14/SmoM2 and Inv/SmoM2/Survivin GOF* mice treated with Survivin inhibitor for 10 days and control mice. **D**, Quantification of the clonal persistence in *SmoM2*-expressing clones an area comprised by 6 groups of triplets of hair follicles in *Krt14/SmoM2* mice treated 4 weeks with SGK1 inhibitor and control mice. (n=number of mice). Statistical significance was assessed using Welch's t test. **E**, Protocol used to induce tumor formation followed by *Survivin* overexpression in *Inv/SmoM2/Survivin GOF* mice. **F G**, Immunostaining for SMOM2 and β4-integrin in *Inv/SmoM2/Survivin GOF* mice treated with tamoxifen followed by doxycycline in preneoplastic stage. Images taken at 8 weeks upon tamoxifen administration. **H**, Quantification of the clone morphology in *Inv/SmoM2/Survivin GOF* mice treated with tamoxifen followed by doxycycline in preneoplastic stage. Quantification performed in samples at 8 weeks upon tamoxifen administration (n=number of mice) test. **I**, Quantification of the clonal persistence in *SmoM2*-expresing clones in an area comprised by 6 groups of triplets of hair follicles in *Inv/SmoM2/Survivin GOF* mice treated first with tamoxifen followed by doxycycline and in controls at 8 weeks upon tamoxifen administration (n=number of mice). Statistical analysis was determined using Welch's t test. Error bars represent the mean ± s.e.m. Scale bar 20 μm in A, B and G and 200 μm in C and G.

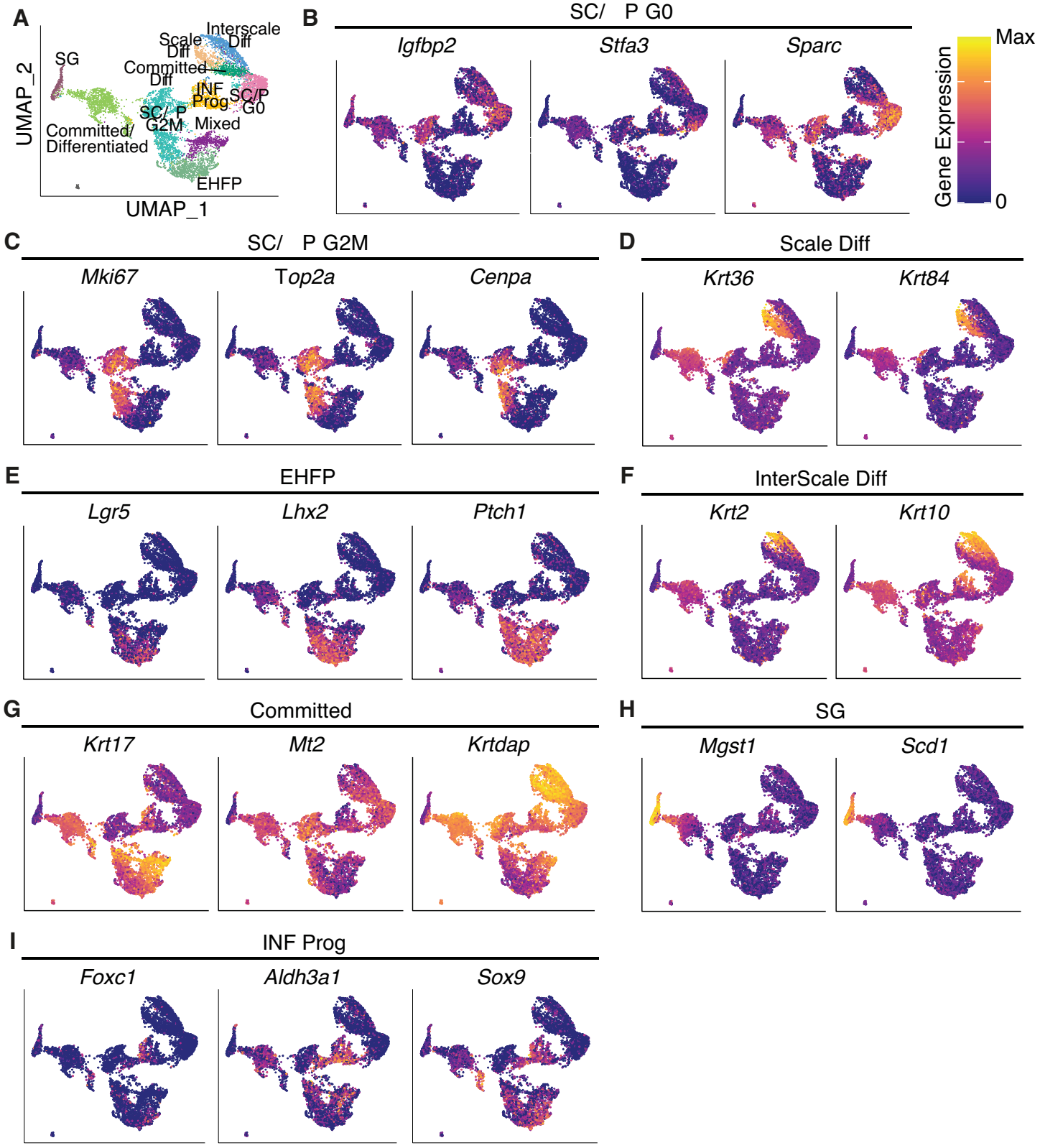

Supplementary Fig. S5 – Annotation for each cell clusters in *Inv/SmoM2* mice. A, Cell clusters found by scRNAseq in *Inv/SmoM2* clones: UMAP dimensionality reduction plots with colors representing unsupervised clustering. **B-I** UMAP plots colored by normalized gene expression for marker genes of (**B**) SC/P G0, (**C**) SC/P G2M, (**D**) Scale differentiation, (**E**) EHFP, (**F**) Interscale differentiation, (**G**) Committed keratinocytes, (**H**) Sebaceous gland and (**I**) Infundibulum progenitor.

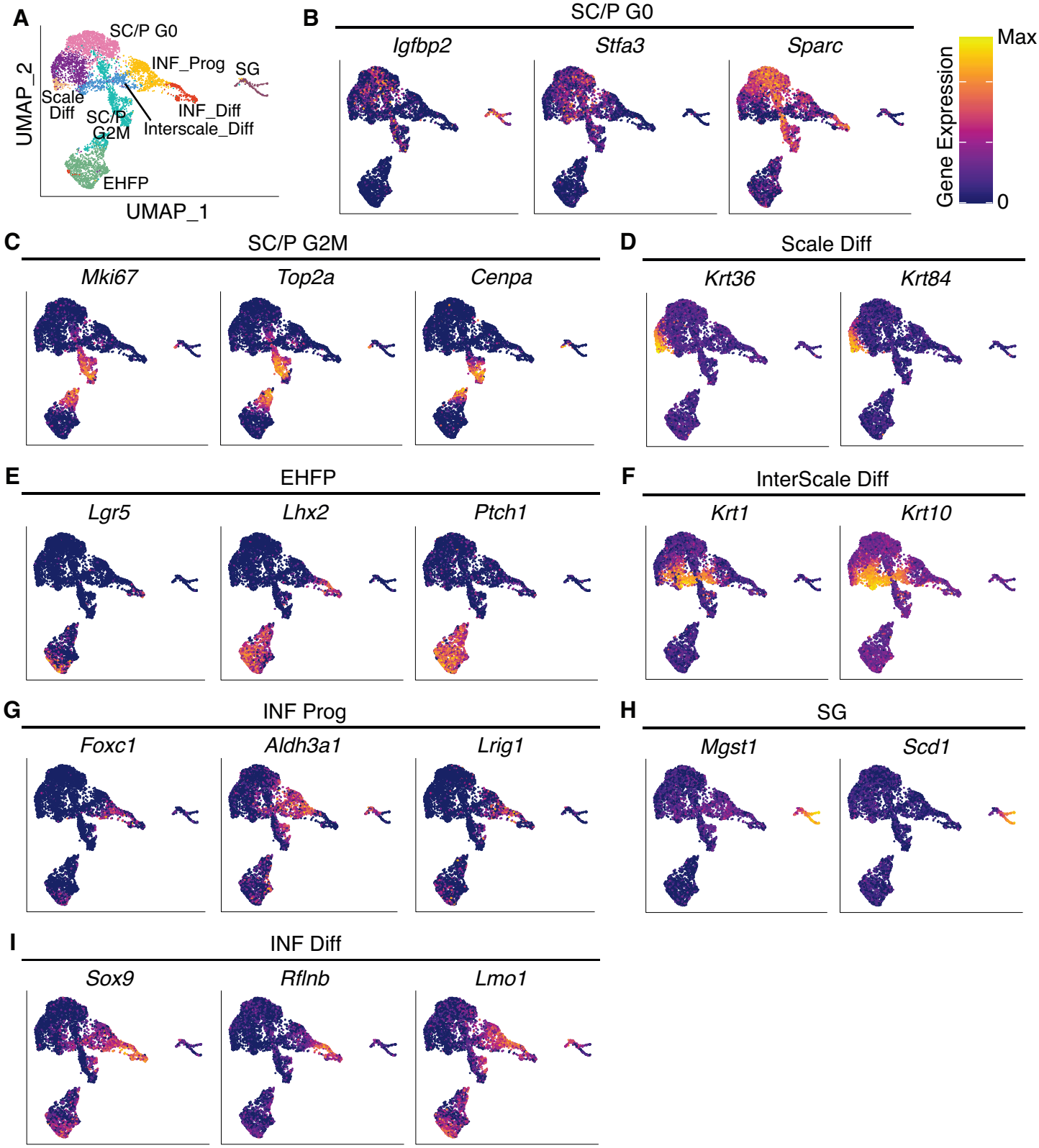

Supplementary Fig. S6 - Annotation for each cell clusters in *Inv/SmoM2/Survivin GOF mice*. A, Cell populations found by scRNAseq in *Inv/SmoM2/Survivin GOF* mice: UMAP dimensionality reduction plots with colors representing unsupervised clustering. **B-I**, UMAP plots colored by normalized gene expression for marker genes of (**B**) SC/P G0, (**C**) SC/P G2M, (**D**) Scale differentiation, (**E**) EHFP, (**F**) Interscale differentiation, (**G**) Infundibulum progenitor, (**H**) Sebaceous gland and (**I**) Infundibulum differentiation.

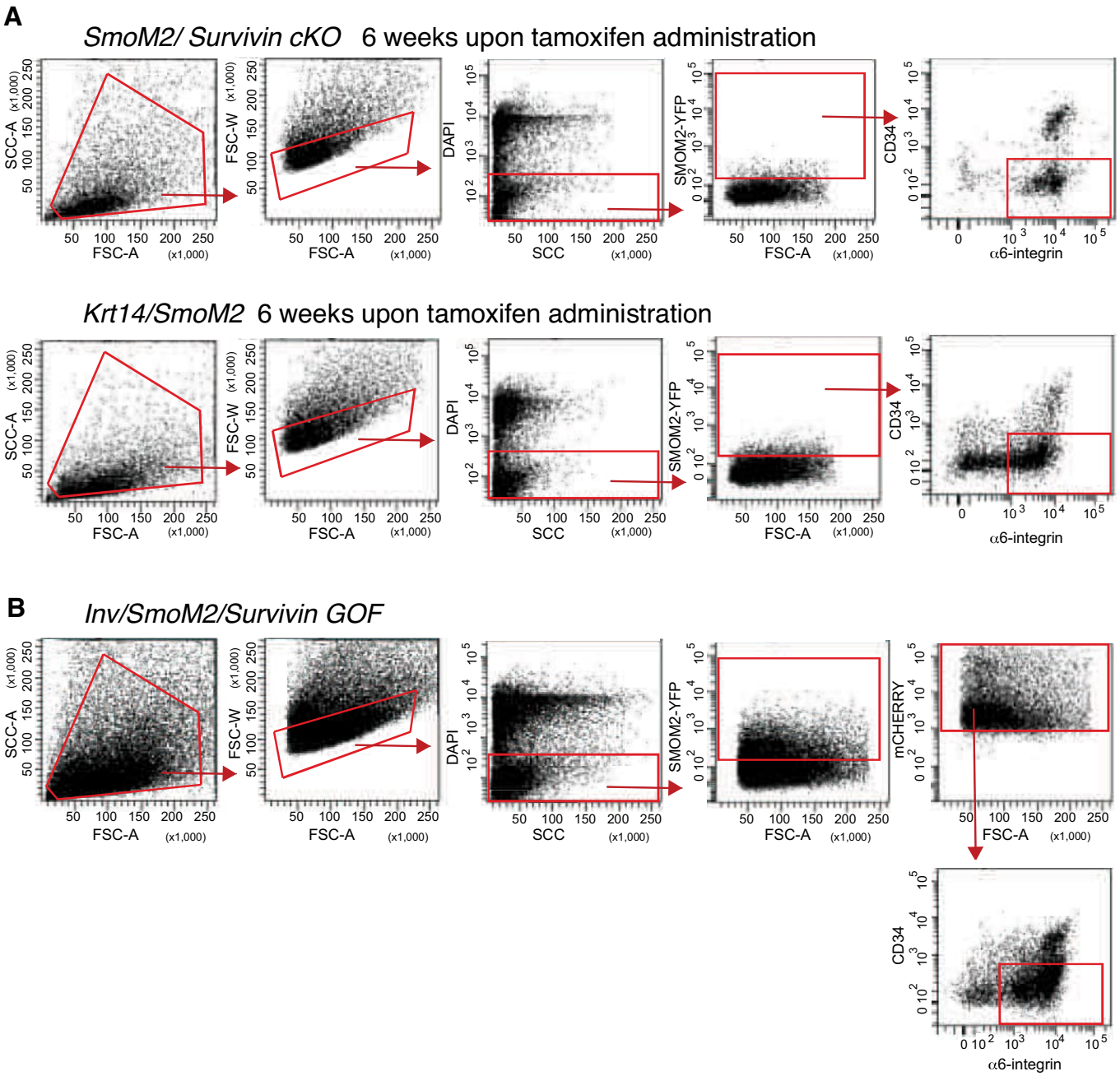

Supplementary Fig. S7 – FACS strategy used to isolate *SmoM2*-expressing cells. **A**, FACS sorting strategy used to isolate *SmoM2*-expressing cells from *Krt14/SmoM2* and *SmoM2/Survivin cKO* mice 6 weeks after tamoxifen administration. Debris were excluded using Forward Scatter (FSC) and side scatter (SCC) and singlets were selected using FSC-W and FSC-A. Live cells were then gated by exclusion of DAPI positive cells. SMOM2-YFP positive cells were gated from the living cells and basal cells located in the interfollicular epidermis – showing high levels of basal marker alpha-6 integrin and no expression of the bulge stem cell marker CD34 - were sorted. **B**, Cell sorting strategy used to isolate *SmoM2*-expressing and SURVIVIN-mCHERRY positive cells from *Inv/SmoM2/Survivin GOF* mice at 8 weeks after tamoxifen administration. The gating strategy used was the same as described in **A**. with the additional step of selection for mCHERRY-expressing tumor cells. A: area; W: width.

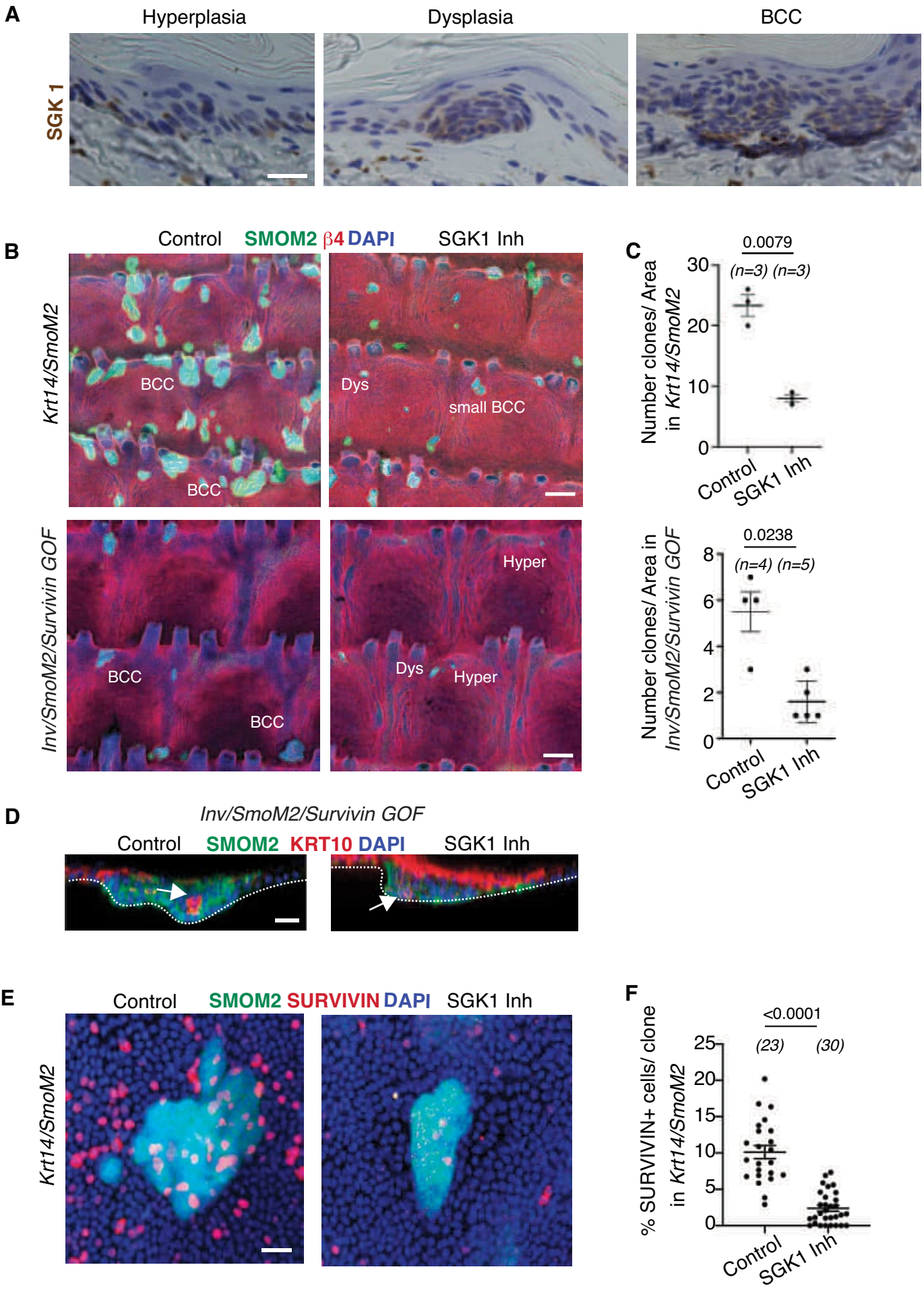

Canato et al, Supplementary Figure S8

Supplementary Fig. S8 – SGK 1 inhibition prevents BCC formation in SCs and Ps expressing SMOM2 and SURVIVIN. A, SGK1 immunohistochemistry in sections from *Krt14/SmoM2* mice. **B**, Image of whole mount showing immunostaining for SMOM2 and β4-integrin in *Krt14/SmoM2* mice treated with SGK 1 inhibitor for 4 weeks and control mice. **C**, Quantification of the clonal persistence in the interscale region of *Krt14/SmoM2* and *Inv/SmoM2/Survivin GOF* control and upon SGK 1 treatment for 4 weeks (n= mice). Statistical analysis was determined using two-way ANOVA test. **D,** Immunostaining for SMOM2 and KRT10 in *Inv/SmoM2/Survivin GOF* lesions 2 weeks upon SGK1 Inhibitor treatment. **E**, Immunostaining for SURVIVIN and SMOM2 in lesions from *Krt14/SmoM2* mice treated for 2 weeks with SGK1 inhibitor. **F**, Quantification of the number of SURVIVIN+ cells per lesion in *Krt14/SmoM2* treated for 2 weeks with SGK1 inhibitor and untreated. Statistical analysis was determined using Mann-Whitney test. Scale bar 200 μm in B and 20um in A, D, E.

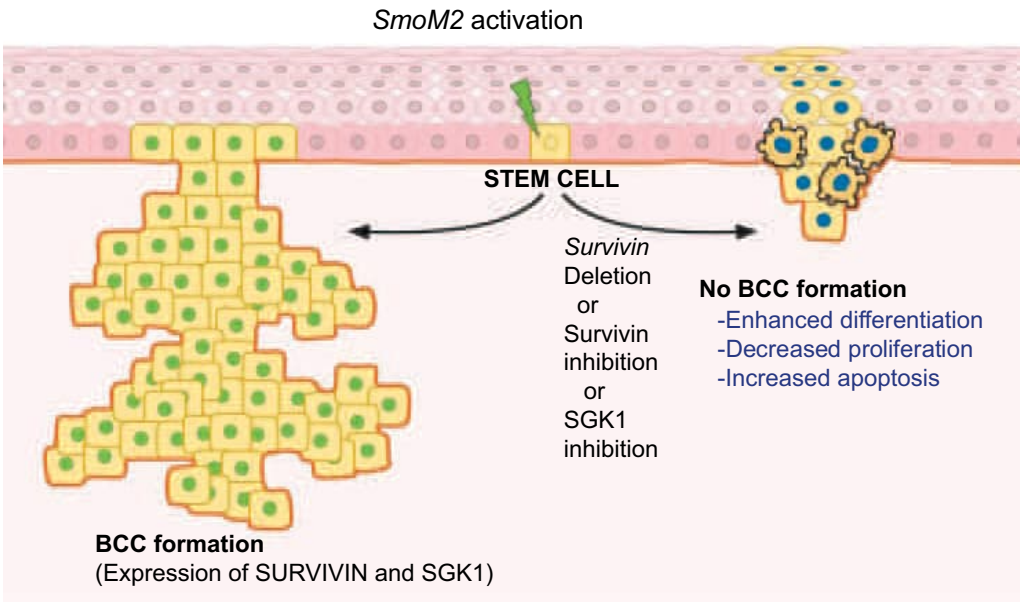

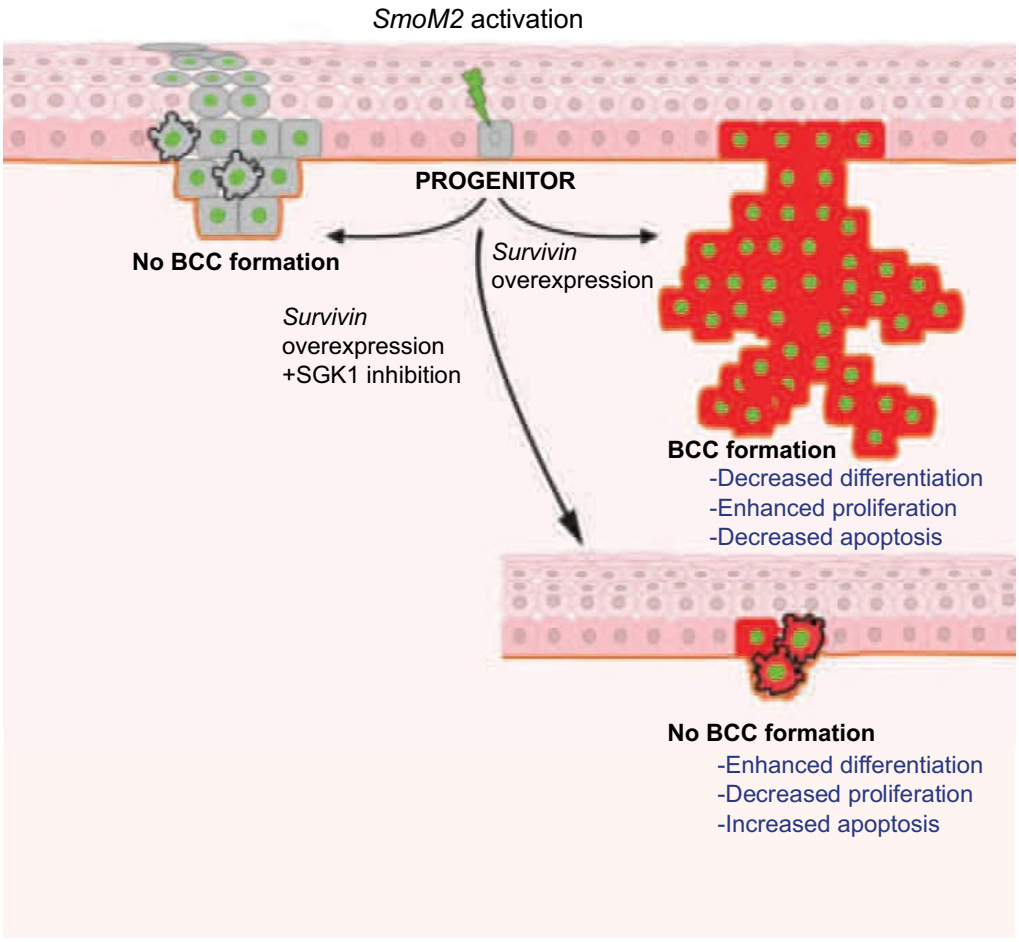

Supplementary Fig. S9 – *Survivin* expression in SCs is essential for BCC initiation. Deletion of *Survivin* in *SmoM2*-expressing SCs prevents BCCs formation by promoting cell differentiation and apoptosis. In contrast, overexpression of *Survivin* in the Ps renders them competent to BCC formation by promoting cell proliferation and survival and preventing differentiation and apoptosis. However, SGK1 inhibition or Survivin inhibition in *SmoM2*- and *Survivin*-expressing Ps and SCs prevents dysplasia from evolving into BCC formation by promoting apoptosis and differentiation while decreasing cell proliferation.